

## A QND measurement of Fock states

D. H. Santamore<sup>y</sup>, A. C. Doherty<sup>y\*</sup>, and M. C. Cross<sup>y</sup><sup>y</sup>Department of Physics, California Institute of Technology, Pasadena, CA 91125 and<sup>\*</sup>Institute for Quantum Information, California Institute of Technology, Pasadena, CA 91125

(dated: February 7, 2020)

We investigate a scheme that makes a quantum non-demolition measurement of the excitation level of a mesoscopic mechanical oscillator by utilizing the anharmonic coupling between two elastic beam bending modes. The non-linear coupling between the two modes shifts the resonant frequency of the readout oscillator proportionate to the excitation of the system oscillator. This frequency shift may be detected as a phase shift of the readout oscillation when driven on resonance. We show that in an appropriate regime this measurement approaches a quantum non-demolition measurement of the phonon number of the system oscillator. As phonon energies in micro-mechanical oscillators become comparable to or greater than the thermal energy, the individual phonon dynamics within each mode can be resolved. As a result it should be possible to monitor jumps between Fock states caused by the coupling of the system to the thermal reservoirs.

PACS numbers: 03.65.Yz, 63.20.Ry

## I. INTRODUCTION

Quantum mechanics tells us that the energy of an oscillator is quantized. However, an observation of quantum limited mechanical motion in macroscopic objects has not been possible because the energy associated with individual phonons is typically much smaller than their thermal energy [1, 2].

Advances in nanotechnology have enabled experimenters to build ever smaller mechanical oscillators with high resonance frequencies and quality factors [3]. As an individual phonon energy becomes comparable to or greater than  $k_B T$ , quantum effects begin to appear and it should be possible to realize various quantum phenomena.

In this paper, we investigate the possibility of observing transitions amongst the Fock states of a mesoscopic mechanical oscillator. To do this requires the coupling of the system oscillator to a measurement device that sensitively detects the phonon number of the system oscillator but does not itself change the excitation level of the oscillator. In the quantum regime it becomes very important to model the precise way that a quantum system interacts with any measuring apparatus, as well as with the environment. Specially, it is necessary to take into account the measurement backaction and to design the system-readout interaction so as to allow the best possible measurement of the desired observable. We will show that it is possible in principle to take advantage of the non-linear interaction between modes of oscillation of an elastic beam or beams to track the state of the oscillator as it jumps between number states due to its coupling to the surrounding thermal environment.

The laws of quantum mechanics tell us that, even in the absence of instrumental or thermal noise, a measurement will tend to disturb the state of the measured system. The interaction between the system and the measurement apparatus means that while information about the measured observable may be read out from the state of the meter after interacting with the system, the quantum mechanical uncertainty in the initial state of the meter leads to random changes in the conjugate observable of the system. This backaction noise on the conjugate observable is an inevitable result of the very interaction that allows the measurement to take place. It has long been recognized that such backaction noise places a fundamental limit on the sensitivity of physical measurements [4]. However, the class of measurements known as quantum non-demolition (QND) measurements partially circumvent this problem by guaranteeing that the backaction noise does not affect the results of future measurements. In a QND measurement the interaction Hamiltonian between system and meter commutes with the internal Hamiltonian of the system: an ideal QND measurement is repeatable since the backaction noise does not affect the dynamics of the measured observable. In this paper, we are interested in a QND measurement of phonon number. The conjugate observable of number is phase, thus, the measurement backaction in our case will result in diffusion of the phase of the mechanical oscillations. However, our scheme allows the complete determination of the oscillator excitation level and thus projects the system onto a number state in an idealized limit.

Our proposed scheme for the QND measurement of phonon number uses two anharmonically coupled modes of oscillation of a mesoscopic elastic structure. The resonant frequencies of these two modes are different. The higher frequency mode is the system to be measured, while the lower frequency oscillator serves as the meter. The key idea of our scheme is that, from the point of view of the readout oscillator, the interaction with the system constitutes a shift in resonance frequency that is proportional to the time-averaged excitation of the system oscillator. This frequency shift may be detected as a change in the phase of the meter oscillations when driven on resonance. We show that this scheme realizes an ideal QND measurement of phonon number in an appropriate limit and discuss the physical

readout regime that is necessary to achieve such a measurement.

In Sec. II we introduce our model and construct the Hamiltonian. Then, in Sec. III, obtain dynamical equations for the system alone by performing an adiabatic elimination of the meter system which has much faster dynamics than that of the system. In Secs. IV and V we change the focus to experimental outcomes based on the system dynamics we have obtained. We first show that the mean and two-point correlation function of the measured quantity reflect the corresponding quantities of the phonon number of the system, We then derive equations of motion for the system conditioned on a particular sequence of measurement results (which yields what is known as a quantum trajectory), and use such results to investigate the possibility of tracking the evolution of the system as it jumps between number states due to its interaction with a thermal bath. We conclude with a discussion of the feasibility of the scheme based on current technology and future enhancements.

## II. CONSTRUCTING THE HAMILTONIAN

### A. The model

In this section we introduce our model system and show how the coupling between the system and meter (or ancilla) approximates a QND coupling in an appropriate limit. We then derive equations of motion that take into account the thermal couplings and the interactions that drive and monitor the oscillations of the readout system.

Consider a mesoscopic beam with rectangular cross section. There are two orthogonal flexing modes that are not coupled in the linear elasticity theory, but are coupled anharmonically. This coupling exists in nature between the two orthogonal flexing modes of single mechanical beam. However, the coupling can also be controlled and engineered: a similar coupling of bending modes in two elastic beams has been proposed by Yurke [5]. In this scheme two mesoscopic elastic beams with rectangular cross section are connected by a series of mechanical coupling devices. These devices have the effect of allowing only one type of strain (the longitudinal stretch) to pass to the other beam. In this paper we focus on the extent to which such mechanical devices are able to realize a QND measurement and the constraints this places on the specifications of the device, and the required temperatures.

For convenience, we refer to the system of interest as oscillator 0 and the ancilla as oscillator 1, and the corresponding resonant frequencies of the two modes as  $\omega_0$  and  $\omega_1$ , respectively. The ancilla is driven at its resonant frequency, and a measurement apparatus is attached to the ancilla. The whole structure is kept at a low temperature such that  $\hbar\omega_0 \gg k_B T$ , where  $\hbar = h/2\pi$  is Planck's constant,  $T$  is the temperature, and  $k_B$  is Boltzmann's constant. The oscillators and the environment are weakly coupled. Figure 1 shows a schematic of our model.

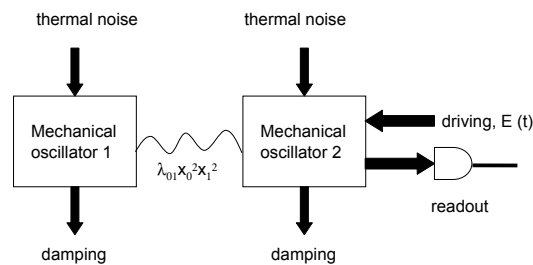


FIG. 1: Schematics of a QND measurement using two coupled mechanical oscillators.

## B. System Hamiltonian

Converting the schematic model in the last section into a realistic mathematical model and obtaining the system dynamics requires some assumptions and simplifications.

Firstly, we focus on the anharmonic coupling and the limit in which it satisfies the QND condition. In linear elasticity theory, two flexing modes, which are perpendicular to each other, propagate independently without interacting. Beyond the linear approximation these modes are coupled. Expansion of the elastic energy with respect to the strain tensor is taken up to second order in the harmonic approximation. The next term, cubic in the elastic energy, gives quadratic terms in the equation of motion [6, 7]. Since the coupling of two flexing modes has a symmetry and they are not coupled at the linear level, the lowest order coupling is  $x_0^2 x_1^2$ . So we expand the anharmonic terms up to first order in coupling and obtain

$$H_{\text{anh}} = \tilde{\sim}_0 x_0^2 + \tilde{\sim}_{00} x_0^4 + \tilde{\sim}_1 x_1^2 + \tilde{\sim}_{11} x_1^4; \quad (1)$$

$$V_{\text{anh}} = \tilde{\sim}_{01} x_0^2 x_1^2; \quad (2)$$

where  $\tilde{\sim}_{ij}$  is the non-linear coupling constant between the oscillators  $i$  and  $j$ , and the expansion of anharmonic terms in each potential is up to the same order as the leading anharmonic coupling term,  $\tilde{\sim}_{01} x_0^2 x_1^2$ . In terms of creation and annihilation operators, the Hamiltonian is

$$H = H_0 + H_{\text{anh}} + V_{\text{anh}}; \quad (3)$$

$$H_0 = \tilde{\sim}!_0 a_0^\dagger a_0 + \tilde{\sim}!_1 a_1^\dagger a_1; \quad (4)$$

$$H_{\text{anh}} = \tilde{\sim}\tilde{\sim}_0 a_0^\dagger + a_0^2 + \tilde{\sim} a_1^\dagger + a_1^2 + \tilde{\sim}\tilde{\sim}_{00} a_0^\dagger + a_0^4 + \tilde{\sim}\tilde{\sim}_{11} a_1^\dagger + a_1^4; \quad (5)$$

$$V_{\text{anh}} = \tilde{\sim}\tilde{\sim}_{01} a_0^\dagger + a_0^2 a_1^\dagger + a_1^2; \quad (6)$$

where we have defined the standard raising and lowering operators for the oscillators  $a_i = \frac{p}{m_i} \frac{\partial}{\partial x_i} + i \sqrt{\frac{m_i}{\hbar \omega_i}} p_i$  and  $a_i^\dagger$  is the Hermitian conjugate of  $a_i$ . Elasticity theory also tells us that the anharmonic coefficients are much smaller than the oscillation frequencies, i.e.,  $\tilde{\sim}!_i \sim \tilde{\sim}_{ij}$  [8]. So far we have ignored any environmental couplings of the two oscillators so as to focus on the interaction of the two oscillators.

The idea of a QND measurement is widely discussed in the literature (for example, see [4], [9], and [10]) and is nicely summarized by Caves et al. [9] as follows: "A measurement which, in principle, can be made time after time on a single system, giving always the same precise result in the absence of external forces (signals). When external forces are present, quantum non-demolition measurements are an ideal tool for monitoring them." Since we want to monitor dynamical changes of  $a_0^\dagger a_0$ , a QND measurement is what we need. In order to perform a QND measurement of  $a_0^\dagger a_0$  the coupling Hamiltonian between the two oscillators  $V$  should satisfy the QND condition

$$[a_0^\dagger a_0; V_{\text{anh}}] = 0; \quad (7)$$

This condition guarantees that the future dynamics of the measured observable  $a_0^\dagger a_0$  are unaffected by the interaction  $V_{\text{anh}}$  with the ancilla.

At this point, it is useful to move into an interaction picture with respect to  $H_0$  in order to determine the regime that approaches the condition in Eq. (7). In the interaction picture with respect to  $H_0$  we find

$$V_{\text{anh}}(t) = \tilde{\sim}\tilde{\sim}_{01} a_0^\dagger e^{i!_0 t} + a_0 e^{i!_0 t} a_1^\dagger e^{i!_1 t} + a_1 e^{i!_1 t} a_0 e^{i!_0 t}; \quad (8)$$

Expanding out the product, there are terms that have the time dependences  $\exp(-i!_0 t)$ ,  $\exp(-i!_1 t)$ , or  $\exp[-i!_0 t - i!_1 t]$ . If the frequencies of the two oscillators satisfy  $!_0 \neq !_1 \sim \tilde{\sim}_{01}$  and  $!_i \sim \tilde{\sim}_{01}$ , then all of these time dependences are very fast relative to the interaction picture time dependence of the state. In this limit the time-dependent terms in  $V_{\text{anh}}(t)$  lead to rapid, small amplitude oscillations of  $a_i$  that essentially average to zero over the time scales for which the non-linearity  $\tilde{\sim}_{01}$  is relevant. If we admit a time coarse-graining and only consider times longer than a mechanical oscillation period we may disregard these time dependent terms; such an approximation is known as the rotating wave approximation (RWA) and is frequently used in quantum optics. Another intuitive explanation for the rotating wave approximation is that the terms with time dependence in the interaction picture drive energy non-conserving transitions, and as long as the condition  $!_0 \neq !_1 \sim \tilde{\sim}_{01}$  is satisfied, the differences in

energy are large and the associated transitions are strongly suppressed as a result. Thus we disregard the energy non-conserving terms in the Hamiltonian to obtain

$$V_{\text{anh}}^{\text{RWA}}(t) = \tilde{\omega}_1 + 2\tilde{a}_1^\dagger a_1 + 2\tilde{a}_0^\dagger a_0 + 4\tilde{a}_0^\dagger a_0 \tilde{a}_1^\dagger a_1 : \quad (9)$$

Note that having made the rotating wave approximation the anharmonic coupling term now commutes with the observable  $\tilde{a}_0^\dagger a_0$ , so a QND measurement can be achieved under the condition  $\tilde{\omega}_0 = \tilde{\omega}_1 + \tilde{\omega}_01$  [37].

The internal anharmonic terms,  $H_{\text{anh}}$ , can be also treated in a similar manner, which result in

$$H_{\text{anh}}^{\text{RWA}} = \tilde{\omega}_0 + 2\tilde{\omega}_0 + 4\tilde{\omega}_00 \tilde{a}_0^\dagger a_0 + 6\tilde{\omega}_00 \tilde{a}_0^\dagger a_0^2 + \tilde{\omega}_1 + 2\tilde{\omega}_1 + 4\tilde{\omega}_11 \tilde{a}_1^\dagger a_1 + 6\tilde{\omega}_11 \tilde{a}_1^\dagger a_1^2 + \tilde{\omega}_3\tilde{\omega}_11 + 3\tilde{\omega}_00 + \tilde{\omega}_0 + \tilde{\omega}_1 : \quad (10)$$

From the Hamiltonian in the rotating wave approximation, we can see that the anharmonic terms cause both a shift in the oscillator resonant frequency and a non-linear phase shift which depends on intensity (a Kerr non-linearity in optical terminology). The constant term can be disregarded since it merely provides an overall phase. We assume that the dominant non-linearity is the coupling given by  $\tilde{\omega}_01$  and disregard the nonlinearities of the system and ancilla internal Hamiltonians [38]. Returning to the Schrodinger picture the Hamiltonian  $H$  now can be written as

$$H^{\text{RWA}} = \tilde{\omega}_0 \tilde{a}_0^\dagger a_0 + \tilde{\omega}_1 \tilde{a}_1^\dagger a_1 + \tilde{\omega}_01 \tilde{a}_0^\dagger a_0 \tilde{a}_1^\dagger a_1; \quad (11)$$

where we have absorbed the corrections to the system and ancilla oscillation frequency into the definition of  $\tilde{\omega}_0$  and  $\tilde{\omega}_1$  and  $\tilde{\omega}_01 = 6\tilde{\omega}_01$ . This Hamiltonian is an adequate description of the dynamics as long as we are not concerned with short times of the order of a mechanical oscillation period.

In the above rotating wave Hamiltonian the excitation of the system oscillator leads to a frequency shift of the ancilla oscillator. Thus it is necessary to monitor the frequency of the ancilla oscillations in order to determine the system excitation. To achieve this we imagine driving the ancilla oscillations on resonance and detecting any shift in phase that is due to the system excitation. There will thus be a driving term on the ancilla that may be written

$$H_{\text{drive}} = 2\tilde{E} \cos \tilde{\omega}_1 t \tilde{a}_1 + \tilde{a}_1^\dagger \quad (12)$$

in the Schrodinger picture, where the parameter  $\tilde{E}$  is used to characterize the strength of the drive. The driving frequency is chosen to resonantly drive oscillations of the ancilla. The phase of the oscillator depends on the frequency of the drive (in-phase below resonance and out-of-phase above resonance). At resonance the phase depends linearly on the driving frequency. If the resonance is shifted due to the system excitation this will be detected as a phase shift between the mechanical oscillations and the drive. In the interaction picture with respect to the ancilla internal Hamiltonian there are again fast oscillating terms that can be neglected in the RWA when  $\tilde{\omega}_1 > \tilde{E}$ . Then we get

$$H_{\text{drive}}^{\text{RWA}} = \tilde{E} \tilde{a}_1 + \tilde{a}_1^\dagger \quad (13)$$

in the interaction picture.

Now we add the coupling of them al baths to the system and ancilla. We employ a standard technique and model the them al baths (the surrounding environment) as an infinite number of harmonic oscillators. The them al baths are linearly coupled to the system (or ancilla) by coordinate-coordinate coupling, i.e.,  $\sum_j A_j x_i x_j$  where  $x_i$  is the system (or ancilla) coordinate,  $x_j$  is the coordinate of an oscillator in the bath, and the index  $j$  corresponds to different bath oscillators. We will again use the rotating wave approximation for the coupling since the couplings are weak.

The nature of the coupling with the measurement instrument depends on what is to be measured. Here we adapt a magnetomotive detection scheme suggested by Yurke et al. [11, 12, 13]. A metallized conducting surface on the ancilla oscillator develops an electromotive force across it due to a perpendicular magnetic field and the oscillation of the beam. The voltage developed depends on

$$V = \mathbb{B} \frac{dx}{dt}; \quad (14)$$

where  $V$  is the voltage,  $\mathbb{B}$  is the magnetic field, the conductor is of length  $l$  and  $x$  is the displacement of the beam from its equilibrium position. Depending on the resistance  $R$  of the conducting strip and remainder of the circuit this will result in a current that is then measured.

In order to quantize this measuring device we follow the standard practice in quantum electronics and model this resistance by a semi-infinite transmission line [14, 15, 16]. The resulting current operator is

$$I(t) / \sum_n b_{d,m}(t) + b_{d,m}^\dagger(t); \quad (15)$$

where  $b_{d,m}(t)$  are the lowering operators for the modes of the transmission line and the proportionality constant, which is not important for our results, depends on the circuit parameters.

The measured current will correspond to measurements of the quantum mechanical observables  $I(t)$ . The experimenter would monitor the amplitude of the resulting signal and its phase with respect to the drive. This signal will include a background of essentially white noise of quantum mechanical and thermal origin. As a result the model describes detection of the motion of the ancilla oscillator with a certain sensitivity that depends on the parameters of the model. In practice the induced voltage of equation (14) would need to be amplified and extra noise must result even in the limit of zero temperature [17, 18, 19]. This does not greatly modify the treatment as it merely reduces the overall sensitivity of the measurement. We will not consider this complication here since we do not wish to focus on technical details of specific measurement schemes but rather on determining the regime in which a QND measurement of phonon number is possible, and the measurement sensitivity that is necessary to track transitions between number states of the system oscillator. Our model should be regarded as a generic quantum mechanical model for measurements with a given sensitivity. A similar analysis will hold for a variety of measurements where the system is linearly coupled to a macroscopic system that determines the measured signal.

For a linearly coupled system-bath measurement within the rotating wave approximation, the Hamiltonian describing the coupling between each measurement current mode and the ancilla is proportional to  $b_{d,m}^\dagger a_1 + b_{d,m} a_1^\dagger$ . The coupling to the thermal baths has the same mathematical structure. In the rotating wave approximation, the difference between a coordinate-coordinate coupling, and a momentum-coordinate coupling can be absorbed into the definition of the phase of the various raising and lowering operators. As is usually done, for later convenience we will include a phase factor of  $\pi/2$  so that the coupling to the baths and measurement current takes the latter form.

The final Hamiltonian for our model is then

$$H = \sum_s \omega_s a_0^\dagger a_0 + \omega a_1^\dagger a_1 + \sum_n \sum_s g_{s,n} b_{s,m}^\dagger b_{s,m} + \sum_n \omega_0 a_0^\dagger a_0 a_1^\dagger a_1 + i \sum_n \gamma_{a_1} a_1^\dagger + i \sum_n D \gamma_{a_1} D^\dagger(t) a_1^\dagger + i \sum_n \gamma_{a_0} a_0^\dagger; \quad (16)$$

where

$$g_{b1} = \sum_n g_{b1,n} b_{b1,m} \quad (17)$$

$$D = \sum_n g_{d,n} b_{d,m} \quad (18)$$

$$g_{b0} = \sum_n g_{b0,n} b_{b0,m}; \quad (19)$$

and the index  $s$  denotes three different baths: the thermal bath coupled to the system ( $b0$ ), the thermal bath coupled to the ancilla ( $b1$ ), and the measurement bath coupled to the ancilla ( $d$ ). The coupling to the bath modes is given by the coefficients  $g_s(n)$ . Later, we will derive the relationship between these coefficients and the corresponding oscillator damping rates or  $Q$ -factors.

We use the dynamics described by Eq. (16) to understand the measurement process. The next section proceeds in the following sequence. Firstly, we find a master equation that describes the evolution of the system and ancilla alone without explicitly describing the state of the environment. Secondly we further simplify this equation by making use of the difference in time-scales between the system and ancilla to obtain a master equation for the system oscillator alone by means of adiabatic elimination. This allows us to determine the effect of the QND measurement coupling on the system.

### III. DYNAMICS OF THE SYSTEM

#### A. Master equation

In this section we present the evolution equations for the ancilla and system alone, tracing out the environmental couplings. We treat the interaction between the oscillators and the environment in the Markov and rotating wave approximations. This is consistent with our treatment of the internal Hamiltonian and we leave it to future work to consider effects beyond the rotating wave regime. The rotating wave approximation is usually very well satisfied in optical systems where non-linear couplings or loss rates are many orders of magnitude smaller than optical frequencies. The difference of time scales will be smaller in the present case but mechanical oscillators with high  $Q$ -factors are becoming realizable in practice and it is in this limit that a QND detection of phonon number will become possible. The starting point for the derivation is the Hamiltonian Eq. (16).

##### 1. Thermal coupling component of the master equation

We first consider a single thermal bath coupled to a system with oscillator with operators  $a_0^\dagger, a_0$ , and then extend the formalism to several baths coupled to both system and ancilla.

We integrate out the bath degrees of freedom using a rotating wave approximation that is widely discussed in the quantum optics literature. We follow the work of Walls and Milburn [10]. This treatment considers the limit of a continuous density of states  $\rho(\omega)$  for the bath operators, which are then treated in second order perturbation theory, assuming that the coupling constant  $g(\omega)$  and  $\rho(\omega)$  vary smoothly around the system oscillation frequency  $\omega_0$ . The bath is assumed to be in a thermal state giving the following correlations for the bath operators

$$\langle b(\omega) b(\omega') \rangle = \langle b^\dagger(\omega) b^\dagger(\omega') \rangle = 0; \quad (20)$$

$$\langle b(\omega) b^\dagger(\omega') \rangle = \delta(\omega - \omega') (N(\omega) + 1); \quad (21)$$

$$\langle b^\dagger(\omega) b(\omega') \rangle = \delta(\omega - \omega') N(\omega); \quad (22)$$

Here  $N(\omega)$  is the average thermal excitation level of the mode at frequency  $\omega$  given by a Bose-Einstein distribution

$$N(\omega) = \frac{1}{e^{\beta \hbar \omega} - 1}; \quad (23)$$

where  $\beta = 1/k_B T$  with  $T$  the temperature of the bath.

This standard treatment results in a master equation for the density operator describing the state of the system after the bath is traced out, in the form

$$\begin{aligned} \dot{\rho}(t) = & \frac{i}{\hbar} [H^0; \rho(t)] \\ & + (N_0 + 1) 2a_0 a_0^\dagger a_0^\dagger a_0 - a_0^\dagger a_0^\dagger a_0 a_0 + N_0 2a_0^\dagger a_0 a_0 a_0^\dagger - a_0 a_0^\dagger a_0 a_0^\dagger; \end{aligned} \quad (24)$$

where  $H^0$  is the Hamiltonian without system-bath interaction, and we have defined

$$\gamma(\omega) = \rho(\omega) |g(\omega)|^2; \quad (25)$$

Physically  $\gamma(\omega)$  gives the damping rate of the amplitude of oscillation, i.e.,  $\gamma(\omega) = \hbar \omega = 2Q_0^{-1}$  where  $Q_0$  is the oscillator  $Q$ -factor. A reduced density matrix equation like (24) is said to be in Lindblad form.

Our model has three baths, and each system (or ancilla) bath coupling gives the same type of contribution to the master equation as the last two terms in Eq. (24). Thus the master equation for the reduced density operator describing the state of the system and ancilla in the interaction picture is

$$\begin{aligned} \frac{d\rho}{dt} = & \frac{i}{\hbar} [H^0; \rho] \\ & + (N_0 + 1) 2a_0 a_0^\dagger a_0^\dagger a_0 - a_0^\dagger a_0^\dagger a_0 a_0 + N_0 2a_0^\dagger a_0 a_0 a_0^\dagger - a_0 a_0^\dagger a_0 a_0^\dagger \\ & + (N_d + 1) 2a_1 a_1^\dagger a_1^\dagger a_1 - a_1^\dagger a_1^\dagger a_1 a_1 + N_d 2a_1^\dagger a_1 a_1 a_1^\dagger - a_1 a_1^\dagger a_1 a_1^\dagger \\ & + (N_1 + 1) 2a_1 a_1^\dagger a_1^\dagger a_1 - a_1^\dagger a_1^\dagger a_1 a_1 + N_1 2a_1^\dagger a_1 a_1 a_1^\dagger - a_1 a_1^\dagger a_1 a_1^\dagger; \end{aligned} \quad (26)$$

where  $\gamma$  is the system damping rate analogous to Eq. (25)

$$\dot{\rho}_0(\omega) = -\gamma \rho_0(\omega) + \dots \quad (27)$$

and  $\gamma_a, \gamma_b$  are the damping rates of the ancilla amplitude due to the environmental couplings

$$\dot{\rho}_a(\omega) = -\gamma_a \rho_a(\omega) + \dots \quad (28)$$

$$\dot{\rho}_b(\omega) = -\gamma_b \rho_b(\omega) + \dots \quad (29)$$

A gain  $\rho_i(\omega)$  is the density of states of bath  $i$  at frequency  $\omega$ , and  $N_i$  are the Bose-Einstein factors

$$N_0 = \frac{1}{e^{\beta \hbar \omega_0} - 1}; N_1 = \frac{1}{e^{\beta \hbar \omega_1} - 1}; N_d = \frac{1}{e^{\beta \hbar \omega_d} - 1} \quad (30)$$

with  $\beta = (k_B T_i)^{-1}$  with  $T_i$  the temperature of bath  $i$ . (We use the symbol  $N_1$  to reserve the symbol  $N_1$  for later use in this section.)

The master equation Eq. (26) is an evolution equation for the density matrix of the open system formed by the two oscillators. The commutator terms on the first line describe the coherent driving of the ancilla oscillator and the non-linear coupling between the two oscillators in the rotating wave approximation. The remaining terms describe the dissipative interactions with the various baths. The terms containing a factor  $(N_i + 1)$  describe the spontaneous and stimulated emission of phonons into the thermal bath while the ones with  $N_i$  correspond to absorption of phonons from the bath.

Notice that the ancilla is coupled to both the thermal environment and the measurement apparatus and each of these couplings results in analogous emission and absorption terms differing only by coefficients. In principle the environmental and measurement baths can have different temperatures described by  $N_1$  and  $N_d$ , however, the overall width of the ancilla resonance is given by  $\gamma = \gamma_a + \gamma_b$ , and if uncoupled from the system, the ancilla would reach a steady state consistent with a thermal equilibrium with excitation  $N_1 = (N_1 + N_d) = \dots$ . For the purposes of the evolution of the system-ancilla density matrix we do not need to distinguish between effects arising from the coupling to the thermal bath and those that result from the measurement coupling, and we may combine these terms to give

$$\begin{aligned} \frac{d\rho}{dt} = & \frac{i\hbar}{\sim} \left[ H, \rho \right] + \dots \\ & + (N_0 + 1) 2a_0 a_0^\dagger \rho - a_0^\dagger a_0 \rho - \rho a_0^\dagger a_0 + N_0 2a_0^\dagger a_0 \rho - a_0^\dagger a_0 \rho - \rho a_0^\dagger a_0 \\ & + (N_1 + 1) 2a_1 a_1^\dagger \rho - a_1^\dagger a_1 \rho - \rho a_1^\dagger a_1 + N_1 2a_1^\dagger a_1 \rho - a_1^\dagger a_1 \rho - \rho a_1^\dagger a_1 : \end{aligned} \quad (31)$$

The master equation Eq. (31) can in principle be numerically integrated. However we will make some further approximations in order to derive a master equation for the system dynamics alone and show that in some limit the readout system coupling results in the phase diffusion that is required as the backaction for the QND measurement, with no extra noise above this quantum limit. To do this we assume that the ancilla is strongly damped (i.e.,  $\gamma \gg \omega$ ). In this limit the ancilla relaxes rapidly to a state consistent with the instantaneous system state. As a result its dynamics are slaved to the system oscillator and can in fact be eliminated from the equations of motion. This adiabatic elimination is described in the following subsection. The final result of our analysis is Eq. (53) below, and some important consequences of the equation are deduced in Sec. III C.

Note that  $\omega_0, \omega_1$  are the width in frequency of the oscillator resonances, and these widths should be taken into account when assessing the validity of the rotating wave approximation. The rotating wave approximation is only valid if  $\omega_0, \omega_1$  is much greater than the linewidth of the oscillators, i.e.,  $\omega_0, \omega_1 \gg \gamma$ . This condition can be understood as not allowing non-energy-conserving transfers of a phonon between the two oscillators.

## B. Adiabatic elimination

For a strongly damped ancilla ( $\gamma \gg \omega$ ) the ancilla state rapidly relaxes to one that oscillates with a phase determined by the current system phonon number. In the interaction picture this is a displaced thermal state, i.e., a state with variance of position and momentum equal to those of a thermal state and non-zero expectation values of position and momentum consistent with the driving and damping of the oscillator. It will be useful to transform the equations of motion in such a way as to make a perturbative expansion around this steady state. The basic idea is to transform the origin of phase space such that the ancilla steady state for the transformed master equation is a thermal state.

This transformation will essentially remove the driving term in the master equation. The same transformation was utilized by Wiseman and Milburn [20] in their study of a driven harmonic oscillator at zero temperature.

Following Wiseman and Milburn, we use the displacement operator,  $D(\alpha) = \exp(-\alpha a_1^\dagger + \alpha a_1)$  with  $\alpha = iE/\hbar\omega$ . The transformed system state is  $\tilde{\rho} = D(\alpha) \rho D(\alpha)^\dagger$  and we may write the master equation for  $\tilde{\rho}$ :

$$\begin{aligned} \dot{\tilde{\rho}} &= D(\alpha) \left[ -\frac{i}{\hbar} [H, \tilde{\rho}] + \gamma_0 \tilde{\rho} + \gamma_1 \tilde{\rho} + (N_0 + 1) 2a_0 \tilde{\rho} a_0^\dagger - \gamma_0 a_0^\dagger \tilde{\rho} - \gamma_0 \tilde{\rho} a_0 + N_0 2a_0^\dagger \tilde{\rho} a_0 - \gamma_0 a_0^\dagger \tilde{\rho} a_0^\dagger - \gamma_0 a_0 \tilde{\rho} a_0 \right. \\ &+ (N_1 + 1) 2a_1 \tilde{\rho} a_1^\dagger - \gamma_1 a_1^\dagger \tilde{\rho} - \gamma_1 \tilde{\rho} a_1 + N_1 2a_1^\dagger \tilde{\rho} a_1 - \gamma_1 a_1^\dagger \tilde{\rho} a_1^\dagger - \gamma_1 a_1 \tilde{\rho} a_1 \left. \right] D(\alpha)^\dagger \end{aligned} \quad (32)$$

In this master equation the ancilla oscillator simply damps towards its displaced origin but the excitation of the ancilla oscillations leads to a frequency shift of the system oscillator described by the first three terms on the right hand side of this equation. The first term is due to the classical mean value of the ancilla oscillator energy and is just a constant shift in the system oscillation frequency. We may move to an interaction picture at this shifted frequency, the most convenient interaction picture in which to perform the adiabatic elimination. The next two terms describe the effect of the fluctuations in the ancilla excitation. The thermal bath coupling terms (the last four groups of terms) in the master equation are the same as before.

We extend the techniques of Wiseman and collaborators [20, 21] to the case of a bath at nonzero temperature by expanding the system-ancilla density matrix perturbatively about the ancilla thermal state. The adiabatic elimination will hold when the ancilla is sufficiently strongly damped, i.e. the terms proportional to  $\gamma_i$  in Eq. (32) dominate in the ancilla dynamics. Thus, the adiabatic elimination is valid in a strongly damped regime such that

$$\frac{\gamma_i}{\omega_i} \gg 1, \quad i = 0, 1 \quad (33)$$

Note that this means we are assuming that the ancilla oscillator relaxes faster than the system oscillator as well as that the non-linear dynamics are weak compared to the damping of the ancilla oscillator. For the consistency of the following treatment it will also be necessary to have  $\gamma_0 N_1 \gg \omega_1^2$ . This requirement follows from the second term (the non-linear coupling term) on the right hand side of the master equation. This constraint can be achieved consistent with Eq. (33), for example, by leaving  $\gamma_0$  finite and choosing  $N_1 \gg \omega_1$ , a regime of low temperature and moderate non-linearity. The approximations are also valid at arbitrary temperature in the limit of strong driving and weak non-linearity such that  $\gamma_0 \gg \omega_1^2$  and  $\gamma_1 \gg \omega_1$  hold [39]. Here the scaling of the driving strength is chosen to preserve the measurement sensitivity which will scale with  $\gamma_0 = \kappa$ . In this regime the frequency shift of the system oscillator becomes large.

As mentioned above the state of the readout oscillator is close to a thermal state about the shifted position and we expand  $\tilde{\rho}$  (with a similar expression for  $\rho$ ) in the form

$$\begin{aligned} \tilde{\rho} &= \rho_0 + \gamma_1^{-1} \rho_1 + \gamma_1^{-2} \rho_2 + \dots \\ &+ \gamma_0^{-2} \rho_0 + \gamma_0^{-3} \rho_1 + \dots \end{aligned} \quad (34)$$

Here the  $\rho_i; i = 0; 1; 2; \dots$  act on the system oscillator with the subscripts indicating orders of magnitude in  $\gamma_i$ . The scalings of the different parameters with  $\gamma_i$  have been chosen to guarantee the consistency of this expansion. The quantity  $\rho_0$  is the thermal density matrix for the ancilla. Note that a term such as  $a_1^\dagger \rho_1$  is off-diagonal in the ancilla number representation, whereas a term such as  $a_1^\dagger \rho_1 a_1$  is diagonal in this basis. The thermal state of an oscillator in terms of the average excitation number  $N_1$  is

$$\rho_0 = \sum_{n=0}^{\infty} \frac{1}{N_1 + 1} \left( \frac{N_1}{N_1 + 1} \right)^n |n\rangle\langle n| \quad (35)$$

We have restricted Eq. (34) to normal ordered terms using the following identities which can be proved from this expression for  $\rho_0$ :

$$a_1^\dagger \rho_0 = \frac{N_1}{N_1 + 1} \rho_0 a_1^\dagger \quad (36)$$

$$\rho_0 a_1 = \frac{N_1}{N_1 + 1} \rho_0 a_1 \quad (37)$$

Using these identities, a term such as  $a_{N_1}^\dagger a_1^\dagger$  and all other anti-normal terms can be expressed in terms of normal ordered terms. Using

$$\begin{aligned} \text{Tr}_1(\rho_{N_1}) &= 1; \\ \text{Tr}_1(a_1^\dagger \rho_{N_1} a_1) &= N_1 + 1; \end{aligned} \quad (38)$$

it can be seen that the system density matrix after tracing out the ancilla state is

$$\rho_s = \text{Tr}_1 \rho_{N_1} = \rho_0 + (N_1 + 1) \rho_2; \quad (39)$$

This form reduces to the form presented by Wiseman and Milburn [20] in the zero temperature limit  $N_1 \rightarrow 0$ . The thermal state in Eq. (35) is the steady state solution of the master equation,  $\dot{\rho} = L_{N_1}[\rho]$ , for an oscillator with lowering operator  $a_1$

$$\begin{aligned} \dot{\rho} = L_{N_1}[\rho] &= (N_1 + 1) 2a_1 a_1^\dagger \rho - a_1^\dagger a_1 \rho - \rho a_1^\dagger a_1 \\ &+ N_1 2a_1^\dagger a_1 \rho - a_1 a_1^\dagger \rho - \rho a_1 a_1^\dagger; \end{aligned} \quad (40)$$

Now we substitute Eq. (34) into Eq. (32) and start to adiabatically eliminate the ancilla operators. The last two terms in Eq. (32) are already in reduced form (i.e., involve the system operators only). We only need to evaluate the remaining terms, which we write as

$$\dot{\rho}_{-0}^P = \frac{\hbar}{i} \rho_{01} a_0^\dagger a_0 - \rho_{10} a_0^\dagger a_0 + 2(N_1 + 1) \rho_{20} + O^3; \quad (41)$$

$$\dot{\rho}_{-1}^P = \frac{\hbar}{i} \rho_{01} a_0^\dagger a_0 [ \rho_{00} + 2 \rho_{20} ] + \frac{\hbar}{i} \rho_{01} \frac{N_1}{N_1 + 1} \rho_{00} + 2 \rho_{20} a_0^\dagger a_0 \rho_{10} + O^3; \quad (42)$$

$$\dot{\rho}_{-1^y}^P = \frac{\hbar}{i} \rho_{01} a_0^\dagger a_0 \frac{N_1}{N_1 + 1} \rho_{00} + \rho_{20} + \frac{\hbar}{i} \rho_{01} [ \rho_{20^y} + \rho_{00} ] a_0^\dagger a_0 \rho_{1^y} + O^3; \quad (43)$$

$$\begin{aligned} \dot{\rho}_{-2}^P &= \frac{\hbar}{i} \rho_{01} a_0^\dagger a_0 \rho_{1^y} + \frac{\hbar}{i} \rho_{01} \frac{N_1}{N_1 + 1} \rho_{10} + \frac{\hbar}{i} \rho_{01} \frac{N_1}{N_1 + 1} \rho_{1^y} + \rho_{10} a_0^\dagger a_0 \\ &+ 2 \rho_{20} - \frac{\hbar}{i} \rho_{01} \frac{N_1}{N_1 + 1} a_0^\dagger a_0; \rho_{00} + O^3; \end{aligned} \quad (44)$$

$$\dot{\rho}_{-2^0}^P = \frac{\hbar}{i} \rho_{01} a_0^\dagger a_0 \rho_{10} - \frac{\hbar}{i} \rho_{01} \frac{N_1}{N_1 + 1} \rho_{10} a_0^\dagger a_0 - 2 \rho_{20} + O^3; \quad (45)$$

$$\dot{\rho}_{-2^0^y}^P = \frac{\hbar}{i} \rho_{01} \frac{N_1}{N_1 + 1} a_0^\dagger a_0 \rho_{1^y} - \rho_{1^y} a_0^\dagger a_0 - 2 \rho_{20^y} + O^3; \quad (46)$$

Notice that all terms that are off-diagonal in the ancilla number basis have the form

$$\dot{\rho}_{-i}^P = \sum_j f(i, j) C_{ij}; \quad (47)$$

where  $i = 1; 2^0$  and  $C = 2$  for  $i = 2^0$  and  $C = 1$  for  $i = 1$ . When  $N_1$  is large, the solution to the above equation quickly decays to the steady state. So we perform adiabatic elimination by setting  $\dot{\rho}_{-2^0} = \dot{\rho}_{-2^0^y} = 0$  and obtain the expressions for  $\rho_{2^0}$  and  $\rho_{2^0^y}$ :

$$\rho_{2^0} = \frac{\hbar}{2} \rho_{01} a_0^\dagger a_0 \rho_{10} - \frac{\hbar}{2} \rho_{01} \frac{N_1}{N_1 + 1} \rho_{10} a_0^\dagger a_0 + O^3; \quad (48)$$

$$\rho_{2^0^y} = \frac{\hbar}{2} \rho_{01} \frac{N_1}{N_1 + 1} a_0^\dagger a_0 \rho_{1^y} - \rho_{1^y} a_0^\dagger a_0 + O^3; \quad (49)$$

Similarly, using Eqs. (48, 49) and setting  $\dot{\rho}_{-1} = \dot{\rho}_{-1^y} = 0$  we find the expressions for  $\rho_{10}$  and  $\rho_{1^y}$ .

$$\rho_{10} = \frac{\hbar}{i} \rho_{01} a_0^\dagger a_0 \rho_{00} - \frac{\hbar}{i} \rho_{01} \frac{N_1}{N_1 + 1} \rho_{00} a_0^\dagger a_0 + O^2; \quad (50)$$

$$\rho_{1^y} = \frac{\hbar}{i} \rho_{01} \frac{N_1}{N_1 + 1} a_0^\dagger a_0 \rho_{00} - \rho_{00} a_0^\dagger a_0 + O^2; \quad (51)$$

We now evaluate the expression Eq. (39) using Eqs. (48)–(51) together with Eqs. (41, 44). After manipulating terms, we obtain

$$\text{Tr}_1 \rho = \frac{\hbar^2 j^2 (2N_1 + 1)}{2} \langle a_0^\dagger a_0; a_0^\dagger a_0; \rangle + O(\hbar^3); \quad (52)$$

Adding back the last two terms in Eq. (32), and using the fact that  $\rho_s = \rho_0 + O(\hbar^2)$ , the reduced master equation becomes

$$\begin{aligned} \dot{\rho}_s = & \frac{\hbar^2 j^2 (2N_1 + 1)}{2} \langle a_0^\dagger a_0; a_0^\dagger a_0; \rangle + \hbar \langle a_0^\dagger a_0; a_0^\dagger a_0; \rangle + \hbar \langle a_0^\dagger a_0; a_0^\dagger a_0; \rangle \\ & + (N_0 + 1) 2a_0 \langle a_0^\dagger a_0; a_0^\dagger a_0; \rangle + N_0 2a_0 \langle a_0^\dagger a_0; a_0^\dagger a_0; \rangle; \end{aligned} \quad (53)$$

A result that follows directly from Eqs. (50,51) is

$$\langle a_1 + a_1^\dagger \rangle = \frac{\hbar j}{2} \langle a_0^\dagger a_0 \rangle; \quad (54)$$

This will be useful later on in evaluating the measured current in terms of system operators.

### C. Decoherence

Equation (53) is the master equation for the system density matrix in the adiabatic approximation, and is the central result of this paper. In the remainder of this section we analyze the physical content of the various terms in this equation, paying particular attention to the effect of the measurement process on the system.

First note that the last two terms in Eq. (53) are associated with the direct system–environment coupling, which may cause transitions between the number states of the system oscillator. We are interested in the possibility of measuring these transitions via the ancilla coupling. The consequences for the system of the coupling to the ancilla, which in turn is coupled to the measurement bath as well as to its thermal bath, are described by the first two terms in Eq. (53). An important feature of these terms is that they represent a QND measurement, since a density matrix that is a pure number state is left unchanged, and the backaction of the measurement does not cause changes in the system number state.

To display the full significance of the first two terms of the master equation (53), let us disregard the system bath (i.e., set  $\gamma = 0$ ) and study a master equation in the form

$$\frac{d\rho_s}{dt} = \hbar \langle a_0^\dagger a_0; a_0^\dagger a_0; \rangle + \hbar \langle a_0^\dagger a_0; a_0^\dagger a_0; \rangle; \quad (55)$$

where

$$\langle a_0^\dagger a_0; a_0^\dagger a_0; \rangle = \hbar \langle a_0^\dagger a_0; a_0^\dagger a_0; \rangle; \quad (56)$$

and

$$\langle a_0^\dagger a_0; a_0^\dagger a_0; \rangle = \frac{\hbar^2 j^2 (1 + 2N_1)}{2}; \quad (57)$$

Equation (55) can be solved explicitly. The equations of motion for the matrix elements in the number representation are

$$\frac{d \langle n | \rho_s | m \rangle}{dt} = \hbar \langle n | a_0^\dagger a_0; a_0^\dagger a_0; | m \rangle - \hbar \langle n | a_0^\dagger a_0; a_0^\dagger a_0; | m \rangle; \quad (58)$$

and the solution to this differential equation is

$$\langle n | \rho_s(t) | m \rangle = \exp[\hbar \langle n | a_0^\dagger a_0; a_0^\dagger a_0; | m \rangle t] \exp[\hbar \langle n | a_0^\dagger a_0; a_0^\dagger a_0; | m \rangle t]; \quad (59)$$

The solution Eq. (59) demonstrates several features: Firstly the result verifies that a pure number state remains unchanged. Secondly, we see that the second term with coefficient  $\hbar \langle a_0^\dagger a_0; a_0^\dagger a_0; \rangle$  in Eq. (55) causes the off-diagonal matrix elements of  $\rho_s$  in the number state basis to decay away to zero. This decay of off-diagonal terms is sometimes known as decoherence. Since the decoherence rate is proportional to  $(n - m)^2$ , terms further from the diagonal decay more rapidly and discussed in Ref. [22]. An alternative way of describing this dynamics is in terms of diffusion of the phase of the oscillator [40]. The first term in Eq. (53) on the other hand yields a frequency shift of the system oscillator due to the mean excitation level of the ancilla. There are two contributions: one from the driving term  $E(a_1 + a_1^\dagger)$  and the second from the thermal excitation  $N_1$  of the ancilla. This means that the QND measurement counts phonons of the mechanical oscillator with the modified oscillation frequency  $\hbar \omega_0 + \hbar^2 j^2 (1 + 2N_1)$ .

## IV. OPERATOR DESCRIPTION OF THE MEASUREMENT

As discussed above, the current  $I(t)$  will be measured experimentally and this signal contains information about the system phonon number because of the interaction between the current and the state of the system oscillator. Specially  $I(t)$  will oscillate at frequency  $\omega_1$  due to the driven oscillations of the ancilla, and we wish to detect a phase shift of this oscillation coming from the energy shift of the ancilla due to the non-linear coupling to the system oscillator. As a result we are interested in the phase quadrature of the component of  $I(t)$  at frequency  $\omega_1$ . In this section we derive expressions for the mean and two point time correlation function of  $I(t)$  and show that these reflect the corresponding quantities of the system occupation number  $a_0^\dagger a_0$ . Thus, at least for low order statistics, the current may be regarded as measuring the phonon number of the system oscillator. Using the techniques of quantum optics for this problem we express the required correlations of the measured signal in terms of correlation functions of the system and ancilla and those that would obtain for an isolated transmission line.

Quantum mechanics also allows us to determine the state of the system conditioned on the measured current  $I(t)$ . The von Neumann projection postulate says that after a measurement a quantum system in some possibly mixed initial state is projected onto the eigenstate corresponding to the measurement outcome. The theory of quantum trajectories [23, 24, 25, 26] has been developed to deal with continuous measurements such as the one we describe here and to determine the state of the system at time  $t$  given the outcomes  $i(t^0)$  of measurements of  $I(t^0)$  for  $t^0$  up to  $t$ . The evolution equation for the conditioned state of the system is derived precisely by projecting the mode corresponding to  $I(t^0)$  onto the appropriate current eigenstate. We discuss such quantum trajectory equations for our system in the next section.

## A. Dynamics of system and bath

In order to calculate the correlation functions of the current, and states of the system and ancilla conditioned on different measurement results, we must write equations of motion in the Markov approximation that do not average over the state of the transmission line. Our discussion essentially parallels the standard quantum optics approach [19, 34]. In particular we follow the treatment in [34] closely. We focus on just the terms involving the ancilla oscillator and the measured bath, in order to relate the correlations of the bath to the correlations of the system. The other degrees of freedom are replaced at the end.

The free Hamiltonian for the ancilla oscillator and the measurement bath is, from Eq. (16),

$$H_{\text{free}} = \omega_1 a_1^\dagger a_1 + \sum_n \omega_{d,n} b_{d,n}^\dagger b_{d,n} \quad (60)$$

where  $b_{d,n}$  is the measurement bath operator and  $a_1$  is the ancilla oscillator operator. The interaction Hamiltonian is, from Eqs. (16) and (18),

$$H_{\text{int}} = i \sum_n g_d(\omega_n) b_{d,n}^\dagger a_1 - b_{d,n} a_1^\dagger \quad (61)$$

where  $g_d(\omega_n)$  is the coupling strength as before. Since the bath is assumed to be large the normal modes of the oscillator are very closely spaced in frequency and we can approximate the spectrum by a continuum. We then wish to write the Hamiltonian in terms of bath operators  $b_d(\omega)$  satisfying the commutation relation

$$[b_d(\omega); b_d^\dagger(\omega')] = \delta(\omega - \omega') \quad (62)$$

In terms of these operators, the sum over modes in the Hamiltonian can be written

$$\sum_n g_d(\omega_n) b_{d,n}^\dagger(t) = \int_0^{\omega_1} \rho_d(\omega) g_d(\omega) b_d^\dagger(\omega) d\omega \quad (63)$$

where  $\rho_d(\omega)$  is the density of states at frequency  $\omega$ .

We may write  $b_d(\omega)$  and  $a_1$  in the interaction picture with respect to  $H_{\text{free}}$  as follows

$$b(\omega; t) = \exp[-i\omega(t - t_0)] b(\omega) \quad (64)$$

$$a_1(t) = \exp[-i\omega_1(t - t_0)] a_1 \quad (65)$$

where  $t_0$  is an initial time at which the interaction and Schrodinger pictures coincide. The Hamiltonian in this interaction picture is then

$$\begin{aligned} H^I(t) &= i \int_{-1}^0 d! \frac{p}{\gamma_d(!)} g_d(!) b_d^y(!;t) a_1(t) - b_d(!;t) a_1(t)^y \\ &= i \int_{-1}^0 d! \frac{p}{\gamma_d(!)} g_d(!) b_d^y(!) a_1 e^{i(!-!_1)(t-t_0)} - b_d(!) a_1^y e^{i(!-!_1)(t-t_0)} \\ &= i \int_{-1}^0 \frac{p}{2} B_t^y a_1 - B_t a_1^y : \end{aligned} \quad (66)$$

where the parameter  $\gamma_d(!) = \gamma_d(!_1)^2$  is the damping rate as defined in the previous section. In the second line we have expressed the interaction picture Hamiltonian in terms of Schrodinger picture operators, which turns out to be convenient. In the final line we define the bath operator  $B_t$  such that

$$B_t = \frac{1}{2 \int_{-1}^0 \gamma_d(!_1) g_d(!_1)} \int_{-1}^0 d! \frac{p}{\gamma_d(!)} g_d(!) b_d(!) e^{i(!-!_1)(t-t_0)} : \quad (67)$$

The bath operator  $B_t$  should be considered to be a linear combination of Schrodinger picture operators, with the phase factors of the coefficients depending on the parameter  $t$ .

In the Markov approximation, which we discussed in the previous section, the coupling to the bath is assumed to be roughly independent of frequency near the resonance  $!_1$ , so  $\gamma_d(!) g_d(!) \approx \gamma_d(!_1) g_d(!_1)$ . The commutation rule for  $B_t$  is

$$\begin{aligned} [B_t; B_t^y] &= \frac{1}{2} \int_{-1}^0 d! \int_{-1}^0 d!^0 b_d(!) b_d^y(!^0) e^{i(!-!_1)(t-t_0)} e^{i(!^0-!_1)(t^0-t_0)} \\ &= \frac{1}{2} \int_{-1}^0 d! e^{i!(t-t_0)} = i(t-t_0) : \end{aligned} \quad (68)$$

In the final line we make the change of variables  $! = !^0 - !_1$  and the approximation of extending the resulting lower limit of the integral  $(-!_1)$  to negative infinity.

As a result of the singular commutator Eq. (68) it is necessary to be careful in integrating the equations of motion determined by  $H^I(t)$ . The time evolution operator is

$$U(t_1; t_0) = T \exp \left[ \int_{t_0}^{t_1} \frac{p}{2} a_1 B_t^y dt^0 - \int_{t_0}^{t_1} a_1^y B_{t^0} dt^0 \right] : \quad (69)$$

where  $T$  represents time-ordering. The operators  $a_1$  factor out of the time integrals since they have no time dependence. In finding the small time limit of the evolution,  $t_1 = t_0 + dt$ , note that the second-order term in perturbation theory is of order  $dt$  because

$$\int_{t_0}^{t_0+dt} B_{t^0} dt^0; \int_{t_0}^{t_0+dt} B_{t^0}^y dt^0 = dt : \quad (70)$$

## B. Current mean and correlations

Consider the current operator  $I$  in Eq. (15). Recall that this is the Schrodinger picture operator describing the current operator located at the ancilla oscillator. It will be useful to move into the Heisenberg picture for the current operator

$$\begin{aligned} I^H(t) &= \exp[iH(t-t_0)] I \exp[-iH(t-t_0)] \\ &= U^y(t; t_0) \exp[iH_0(t-t_0)] I \exp[-iH_0(t-t_0)] U(t; t_0); \end{aligned} \quad (71)$$

where  $U(t; t_0)$  is the interaction picture time evolution equation defined in Eq. (69). We anticipate that the current signal is going to track the oscillations of the ancilla oscillator and thus the dominant signal will be close to  $!_1$ . The system excitation described by  $a_0^y a_0$  will result in a phase shift of the ancilla oscillations and experimentally this could be detected by demodulating  $I(t)$  at frequency  $!_1$ . So in fact we are interested in the low frequency components

of  $\cos[\omega_1(t - t_0)]I^H(t)$ . By changing the sum in Eq. (15) into an integral as before, substituting into Eq. (71) and comparing with the definition of  $B_t$  in Eq. (67) we find

$$\cos[\omega_1(t - t_0)]I^H(t) / U^Y(t; t_0) (B_t + B_t^Y)U(t; t_0) + (\dots): \quad (72)$$

The omitted terms have factors of  $\exp[-i2\omega_1(t - t_0)]$  and will contribute high frequency terms to the signal that we will ignore here; these would be filtered out in any experiment. In other words we are discarding terms in the mean values and correlation functions that we derive below that have fast time dependences; this is necessary for consistency with the Markov approximations we have made in the dynamical equations. For this reason we define the demodulated current operator (in the Heisenberg picture)

$$I_{dm}(t) = U^Y(t; t_0) (B_t + B_t^Y)U(t; t_0); \quad (73)$$

where we have scaled the units of the current to eliminate proportionality constants in this expression. For simplicity of notation, from now on we drop the subscript "dm" denoting the demodulation of the current, and refer to Eq. (73) as "the current". Note that the commutation relations for  $B_t$  imply that the observables at different times are approximately commute.

We can now evaluate  $I(t)$  a little more explicitly. However, it is necessary to be careful of the singular nature of the evolution operator; as a result we consider the time evolution up to a time  $t_1 > t$  and take the limit  $t_1 \rightarrow t$  at the end of the calculation. For  $t_1 > t > t_0$  we can write  $U(t_1; t_0) = U(t_1; t + dt)U(t + dt; t)U(t; t_0)$  and then from the commutation relations Eq. (68) for  $B_t$  and the definition of the evolution operator Eq. (69) it is clear that the time evolution takes place only around time  $t$  since  $[B_t; U(t; t_0)] = 0$  and  $[B_t; U(t_1; t + dt)] = 0$ . Physically this is a result of the Markov approximation: after interacting with the system at time  $t$  the subsequent dynamics of the mode  $B_t$  are unaffected by the interaction. Hence we can write

$$\begin{aligned} B_t(t_1) &= U^Y(t_1; t_0)B_tU(t_1; t_0) \\ &= U^Y(t; t_0) (B_t + \frac{P}{2} a_1)U(t; t_0) \\ &= B_t + \frac{P}{2} U^Y(t; t_0)a_1U(t; t_0); \end{aligned} \quad (74)$$

Note that  $B_t(t_1)$  defined by this expression for  $t_1 > t$  is in fact independent of the time  $t_1$ , and so we may write it simply as  $B_t$ . To derive this result, in the second line we used  $U(t_1; t_0) = U(t_1; t + dt)U(t + dt; t)U(t; t_0)$ , commuted  $U(t_1; t + dt)$  through  $B_t$ , expanded  $U(t + dt; t)$  to first order and employed the commutation relations Eq. (68). In the third line we use the fact that  $[U(t; t_0); B_t] = 0$ . Recall that  $B_t$  is a Heisenberg picture operator so expectation values should be taken against the initial state  $|\psi(t_0)\rangle$ . This is convenient since the modes of the bath are initially assumed to have thermal statistics so expectation values of the first term are easy to evaluate. On the other hand

$$\text{Tr}[U^Y a_1 U(t; t_0) |\psi(t_0)\rangle] = \text{Tr}[a_1^{-1}(t)] = \exp[i\omega_1(t - t_0)] \langle a_1(t) \rangle \quad (75)$$

where  $^{-1}(t)$  is the interaction picture density matrix of the system. As we wished the demodulation has picked out the component of the signal oscillating at  $\omega_1$ . Since our master equations evolve the system state in the interaction picture this is the most convenient form for the expression for  $B_t$ . The demodulated current operator can then be written in terms of these operators

$$I(t) = B_t + B_t^Y :$$

We now proceed to evaluate the correlations of the demodulated current in terms of the correlation functions of the system oscillator calculated from the interaction picture master equation. As before we have assumed that the bath is in equilibrium at some temperature determined by  $N_1$  so

$$\langle B_t^Y \rangle = \langle B_t \rangle = 0; \quad (76)$$

so the average current is

$$\langle I(t) \rangle = \frac{P}{2} \langle a_1 + a_1^Y \rangle : \quad (77)$$

Where we have adopted the shorthand notation  $\langle a_1 + a_1^Y \rangle(t) = \text{Tr} [a_1 + a_1^Y]^{-1}(t)$ . Using Eq. (54) gives us the relationship that shows that the mean current is indeed a measure of the mean system phonon number

$$\langle I(t) \rangle = \frac{8}{2} \sum_{j=1}^2 \langle a_{0j}^Y a_0 \rangle(t); \quad (78)$$

## C . Current correlation

We now find the two time current correlations,

$$\begin{aligned} \langle I(t^0) I(t) \rangle &= \langle \mathcal{B}_{t^0}^D + \mathcal{B}_{t^0}^E \mathcal{B}_t^D + \mathcal{B}_t^E \mathcal{B}_{t^0}^D + \mathcal{B}_t^E \mathcal{B}_t^E \rangle \\ &= \langle \mathcal{B}_{t^0}^D \mathcal{B}_t^D + \mathcal{B}_{t^0}^E \mathcal{B}_t^E + \mathcal{B}_{t^0}^D \mathcal{B}_t^E + \mathcal{B}_{t^0}^E \mathcal{B}_t^D \rangle \end{aligned} \quad (79)$$

In order to evaluate the different terms here we use the results of Gardiner and Collett ([19] p168) to express these correlation functions in terms of normally and anti-normally ordered correlation functions of the ancilla observables :

$$\langle \mathcal{B}_{t^0}^D \mathcal{B}_t^E \rangle = (N_d + 1) \langle a_1(t^0) a_1(t) \rangle \quad \langle \mathcal{B}_{t^0}^E \mathcal{B}_t^D \rangle = N_d \langle a_1(t^0) a_1(t) \rangle ; \quad (80)$$

$$\langle \mathcal{B}_{t^0}^D \mathcal{B}_t^D \rangle = (N_d + 1) \langle a_1^y(t^0) a_1(t) \rangle \quad \langle \mathcal{B}_{t^0}^E \mathcal{B}_t^E \rangle = N_d \langle a_1(t^0) a_1^y(t) \rangle + N_d \langle a_1(t^0) a_1(t) \rangle ; \quad (81)$$

$$\langle \mathcal{B}_{t^0}^E \mathcal{B}_t^D \rangle = (N_d + 1) \langle a_1^y(t) a_1(t^0) \rangle \quad \langle \mathcal{B}_{t^0}^D \mathcal{B}_t^E \rangle = N_d \langle a_1(t^0) a_1^y(t) \rangle + (N_d + 1) \langle a_1(t^0) a_1(t) \rangle ; \quad (82)$$

$$\langle \mathcal{B}_{t^0}^E \mathcal{B}_t^E \rangle = (N_d + 1) \langle a_1^y(t^0) a_1^y(t) \rangle \quad \langle \mathcal{B}_{t^0}^D \mathcal{B}_t^D \rangle = N_d \langle a_1^y(t^0) a_1^y(t) \rangle ; \quad (83)$$

where  $T$  and  $\bar{T}$  are time and anti-time ordering, respectively.

Each of the ancilla correlation functions in the above equations is with respect to the interaction picture evolution. So for arbitrary operators  $X$  and  $Y$  the correlation functions should be interpreted as

$$\langle X(t) Y(t^0) \rangle = \text{Tr} U^y(t; t^0) X U(t; t^0) U^y(t^0; t^0) Y U(t^0; t^0) \rho(t^0) \quad (84)$$

Since we are interested in the case where the operators  $X$  and  $Y$  do not act on the bath it is possible to use the cyclic properties of the trace to express these in terms of the master equation

$$\begin{aligned} \langle X(t) Y(t^0) \rangle &= \text{Tr}_{\text{sys+anc}} X \text{Tr}_{\text{bath}} U(t; t^0) Y U(t; t^0) \rho(t^0) U^y(t; t^0) U^y(t+; t) \\ &= \text{Tr}_{\text{sys+anc}} (X \exp[L] Y(t) g) \end{aligned} \quad (85)$$

where  $\rho(t^0)$ . After the bath trace leading to Eq. (85),  $\rho(t)$  is the reduced density operator of the system and ancilla in the interaction picture and the time evolution is the Lindblad form  $\exp[L]$  corresponding to the solution of the of the master equation (31).

In the time anti-ordered case we find, similarly,

$$\langle X(t) Y(t+) \rangle = \text{Tr} Y \exp[L] \rho(t) X \quad (86)$$

We then have, again for  $t > 0$ ,

$$\begin{aligned} \langle I(t+) I(t) \rangle &= (N_d + 1) \langle a_1(t+) a_1(t) \rangle \quad \langle \mathcal{B}_{t^0}^D \mathcal{B}_t^E \rangle = N_d \langle a_1(t) a_1(t+) \rangle \\ &+ (N_d + 1) \langle a_1^y(t) a_1(t+) \rangle \quad \langle \mathcal{B}_{t^0}^E \mathcal{B}_t^D \rangle = N_d \langle a_1(t+) a_1^y(t) \rangle + (N_d + 1) \langle a_1(t) a_1(t+) \rangle \\ &+ (N_d + 1) \langle a_1^y(t+) a_1(t) \rangle \quad \langle \mathcal{B}_{t^0}^D \mathcal{B}_t^E \rangle = N_d \langle a_1(t) a_1^y(t+) \rangle + N_d \langle a_1(t) a_1(t+) \rangle \\ &+ (N_d + 1) \langle a_1^y(t) a_1^y(t+) \rangle \quad \langle \mathcal{B}_{t^0}^E \mathcal{B}_t^E \rangle = N_d \langle a_1^y(t+) a_1^y(t) \rangle \end{aligned} \quad (87)$$

We will now indicate how to evaluate the different correlations functions in this equation in terms of correlation functions of system observables in the adiabatic approximation.

Consider for example  $\langle a_1^y(t+) a_1(t) \rangle$ , which can be written

$$\langle a_1^y(t+) a_1(t) \rangle = \text{Tr} a_1^y \exp[L] f a_1(t) g \quad (88)$$

We define

$$f(t) = a_1(t); \quad (89)$$

$$g(t+) = \exp[L] f a_1(t) g; \quad (90)$$

Note that  $\rho(t)$  is not Hermitian and does not have unit trace, and so it is not a valid density matrix. However, it has the same equation of motion as  $\rho(t)$ , and the adiabatic elimination of the fast ancilla degrees of freedom will proceed as in Sec. III B. The idea of the calculation is then to regard  $\rho(t)$  as the initial condition for the time evolution. The expansion of  $\rho(t)$  about the thermal state of the ancilla in Eq. (34) leads to a similar expansion for  $\rho(t)$ . We then use the adiabatic approximation for the dynamics as in Sec. III B to write the off-diagonal terms in this expansion at time  $t + \tau$  in terms of the diagonal terms. This requires that  $\tau \gg \tau_c$ ; correlations on a shorter time scale than this would require going beyond the adiabatic approximation. We then write the evolution of the diagonal terms in terms of the adiabatically eliminated master equation and the initial condition  $\rho(t)$ , and finally express the result in terms of correlations of the system oscillator.

First consider  $\rho(t) = a_1^\dagger(t) a_1(t)$  using Eq. (34),

$$\rho(t) = \rho_0(t) + \frac{N_1}{1+N_1} \rho_1(t) + \frac{N_1^2}{(1+N_1)^2} \rho_2(t) + \dots \quad (91)$$

For sufficiently long  $\tau$  the off-diagonal terms will again be slaved to the on-diagonal terms. Expanding  $\rho(t + \tau)$  as in the same way  $\rho(t)$ ,

$$\rho(t + \tau) = \rho_0(t + \tau) + \frac{N_1}{1+N_1} \rho_1(t + \tau) + \frac{N_1^2}{(1+N_1)^2} \rho_2(t + \tau) + \dots \quad (92)$$

So the correlation function is

$$\langle a_1^\dagger(t + \tau) a_1(t) \rangle = (N_1 + 1) \text{Tr}_{\text{sys}} [\rho_1(t + \tau)]; \quad (93)$$

where we have used Eq. (38). In the adiabatic approximation we may write  $\rho_1(t + \tau)$  in terms of  $\rho_0(t + \tau) = \rho_s(t + \tau) + O(\tau^{-2})$  using Eq. (51). We obtain

$$\text{Tr}_{\text{sys}} [\rho_1(t + \tau)] = (N_1 + 1) \text{Tr}_{\text{sys}} [e^{-\tau L_{\text{sys}}} a_0^\dagger a_0 \rho_s(t)]: \quad (94)$$

Finally we know that the reduced density matrix of the system has evolved under the adiabatically eliminated master equation (53) so that  $\rho_s(t + \tau) = \exp(L_{\text{sys}} \tau) \rho_{\text{anc}} a_1^\dagger(t) a_1(t) g$ . Evaluating  $\rho(t) = a_1^\dagger(t) a_1(t)$  from Eq. (91) gives for the trace

$$\text{Tr}_{\text{anc}} \rho(t) = (N_1 + 1) \rho_1(t); \quad (95)$$

Finally, using Eq. (50) gives the result for the correlation function

$$\begin{aligned} \langle a_1^\dagger(t + \tau) a_1(t) \rangle &= \text{Tr}_{\text{sys}} [e^{-\tau L_{\text{sys}}} a_0^\dagger a_0 \exp(L_{\text{sys}} \tau) e^{-\tau L_{\text{sys}}} (N_1 + 1) a_0^\dagger a_0 \rho_s(t) + O(\tau^3)] \\ &= \frac{\tau^2}{2} \langle a_0^\dagger a_0 \rangle^2 \text{Tr}_{\text{sys}} [e^{-\tau L_{\text{sys}}} a_0^\dagger a_0 \rho_s(t) a_0^\dagger a_0 \rho_s(t) + O(\tau^3)]; \end{aligned} \quad (96)$$

where we have again used  $\rho_s = \rho_0 + O(\tau^{-2})$  and the expression for  $\rho_1(t)$  in terms of  $\rho_0(t)$ . The other terms in equation (87) are calculated in an exactly similar way so we omit them here.

Proceeding with the rest of the correlation gives the rest of the time-ordered correlation functions below:

$$\langle a_1^\dagger(t) a_1^\dagger(t + \tau) \rangle = \langle a_1^\dagger(t + \tau) a_1^\dagger(t) \rangle \quad (97)$$

$$\begin{aligned} \langle a_1^\dagger(t + \tau) a_1^\dagger(t) \rangle &= \langle a_1^\dagger(t) a_1^\dagger(t + \tau) \rangle \\ &= \frac{\tau^2}{2} \langle a_0^\dagger a_0 \rangle^2 (1 + N_1) \langle a_0^\dagger a_0(t) a_0^\dagger a_0(t + \tau) \rangle + O(\tau^3) \end{aligned} \quad (98)$$

$$\begin{aligned} \langle a_1^\dagger(t + \tau) a_1(t) \rangle &= \langle a_1^\dagger(t) a_1(t + \tau) \rangle \\ &= \frac{\tau^2}{2} \langle a_0^\dagger a_0 \rangle^2 N_1 \langle a_0^\dagger a_0(t + \tau) a_0^\dagger a_0(t) \rangle + O(\tau^3) \end{aligned} \quad (99)$$

$$\begin{aligned} \langle a_1^\dagger(t + \tau) a_1(t) \rangle &= \langle a_1^\dagger(t) a_1^\dagger(t + \tau) \rangle \\ &= \frac{\tau^2}{2} \langle a_0^\dagger a_0 \rangle^2 N_1 \langle a_0^\dagger a_0(t) a_0^\dagger a_0(t + \tau) \rangle + O(\tau^3) \end{aligned} \quad (100)$$

Finally for the phase of the driving we have assumed where  $\epsilon = iE = \dots$ , is purely imaginary, and so we can write the result for the current correlations as

$$\langle I(t+\tau) I(t) \rangle = 2 \frac{\hbar^2 J^2}{\omega_0^2} a_0^\dagger a_0(t+\tau) a_0^\dagger a_0(t) + (1 + 2N_1) \dots \quad (101)$$

Note that the second order time correlation function of the current is proportional to the time-symmetric correlation function of the system phonon number, with in addition a white noise  $\delta$ -function term. (In thermal equilibrium the system number correlations would be time symmetric, but this is not necessarily true otherwise). Hence, not only the mean value but also the second-order statistics of the current are simply related to the system phonon number. This result shows that in the adiabatically eliminated regime the measured current does indeed provide a measurement of phonon number.

## V. QUANTUM TRAJECTORIES

In this section we derive an equation of motion for the state of the system conditioned on a particular sequence of measurement outcomes. This equation is termed a quantum trajectory, and results from continually projecting onto eigenstates of the current. Since the current effectively measures phonon number, this measurement process will tend to force the system towards a pure number state that is consistent with the measurement current. The time scale for this to occur will depend on the coupling of the system to the measurement apparatus, which is in turn connected to the sensitivity of the measurement. On the other hand, the coupling of the system to a thermal bath will lead it to absorb and emit energy from the bath. Thus, in order to determine which number state the system is in and track its evolution, it must be possible to distinguish between one number state and the next in a time that is short compared to the time scale over which phonons are absorbed from and emitted into the thermal bath.

After discussing some background on quantum trajectory equations, we derive the appropriate trajectory equation for our setup, and discuss the regime of sensitivity and temperature in which we expect to be able to track the phonon number.

### A. Background

Quantum trajectories give a method for us to calculate the state of the system conditioned on the measured current [23, 24, 25, 26]. A quantum trajectory is constructed as follows. Over each infinitesimal time interval, the system and current bath states become weakly entangled via the interaction Hamiltonian. As a consequence, at each time instant, the state of the system influences the distribution of the possible values of the current  $I$  that may be obtained in the measurement. In turn, von Neumann projections of the entangled states allow us to calculate the effect of the measurement on the system state. The appropriate projection is onto the current eigenvector corresponding to the measured current value. This results in a stochastic master equation for the state evolution. To implement the quantum trajectory approach we perform a simulation by picking the measurements  $I(t)$  from the correct probability distribution and following the corresponding evolution of the system state. The  $I(t)$  curve produced by a simulation is representative of a single experimental run, and is a useful predictor of what the experimenter might see. There will be a signal contribution that reflects the system state, as well as a white noise background arising from both thermal and quantum noise. The result for the density matrix, on the other hand, describes the ensemble of all experiments consistent with the initial conditions and the particular  $I(t)$ .

It is also interesting to mention that such stochastic simulations of idealized measurements are often performed for numerical reasons in quantum optics, since it is possible to calculate the trajectories corresponding to imaginary measurements for which the conditioned state is always pure. Mean values or correlation functions may then be found by averaging over many trajectories [19]. Pure states take less memory to store and less computation to update than the mixed density matrix that appears in the master equation. Thus the trajectory method is often more efficient than the direct integration of the master equation. As long as the objective of a quantum trajectory calculation is solely to obtain the solution to a master equation, there are a number of different stochastic master equations that may be used. These are known as unravelling of the original master equation. However, when a trajectory is used to infer the state of the system conditioned on the outcome of an individual experiment, the stochastic master equation must be determined from the physics associated with the actual measurement. Since our detection scheme uses electrical current, the appropriate unravelling corresponds to projecting onto current eigenstates.

There are a number of review and tutorial articles on quantum trajectories available for the interested reader (see for example, [27] and [28]).

## B. Description of the measurement

In Sec. II B, we introduced the bath operator Eq. (67)

$$B_t = \frac{1}{2} \sum_d \gamma_d \rho_d \int_0^t dt' e^{i(\omega_d - \omega_s)(t-t')} \rho_d \rho_d^\dagger \quad (102)$$

which satisfies the commutation rule  $[B_t, B_t^\dagger] = \hbar \delta(t-t')$  in the Markov approximation.

We will follow Wiseman's discussion (Ref. [26], x 4.4.1) of homodyne detection in quantum optics, which maps onto the same form of Hamiltonian as ours. Note when comparing with Ref. [26], that Wiseman uses a different scaled form of the current.

The idea of the calculation is to consider the interaction of the ancilla with the bath at time  $t$ , represented by the operator  $B_t$ , over a small time interval  $\delta t$ . It is supposed that each "element" in the time sequence of the bath  $B_t$  is initially described by a thermal state. Over the interval  $\delta t$  the ancilla and bath states become weakly correlated. Measurement of the current (i.e., the bath operator  $B_t + B_t^\dagger$ ) then finds a value of the current equal to an eigenvalue  $I$  of the current operator, with the corresponding eigenstate  $|j\rangle$ , with a probability distribution  $P(I)$  given by the density matrix of the entangled state in the usual way.

$$P(I) = \langle j | (B_t + B_t^\dagger) | j \rangle \quad (103)$$

The measurement also projects the density matrix onto the eigenstate  $|j\rangle$

$$\rho \rightarrow \frac{|j\rangle \langle j| \rho (B_t + B_t^\dagger) |j\rangle \langle j|}{\langle j | (B_t + B_t^\dagger) | j \rangle} \quad (104)$$

Since the value of the current measured is a stochastic variable, this projection adds a stochastic component to the evolution of the density matrix.

To follow the evolution over a time  $t$  it is useful to introduce the normalized operator

$$B = \int_0^t dt' B_t dt' = \int_0^t dt' B_t dt' \quad (105)$$

which satisfies the commutation rule

$$[B(t), B^\dagger(t')] = \hbar \delta(t-t') \quad (106)$$

With this notation we can now formulate the ancilla-bath entangling and measurement process. At time  $t$  the density matrix representing the ancilla and the segment of the measurement bath represented by  $B(t)$  can be written as a direct product of the system plus ancilla  $\rho_s(t)$  and bath  $\rho_b(t)$  density matrices

$$\rho(t) = \rho_s(t) \otimes \rho_b(t); \quad (107)$$

and  $\rho_b(t)$  is a thermal state. The interaction Hamiltonian in terms of the operators  $B_t; B_t^\dagger$  is from Eqs. (61) and (66),

$$H_{int} = i \frac{\hbar}{2} (B^\dagger(t) a_1 - B_t a_1^\dagger); \quad (108)$$

with  $\gamma_d \rho_d \rho_d^\dagger$  the damping rate as in Eq. (27). Then, to lowest order the evolution under the interaction gives

$$\rho(t + dt) = \rho_s(t) \otimes \rho_b(t) + \frac{\hbar}{2} \int dt' B^\dagger(t') a_1 - a_1^\dagger B_t; \rho_s(t) \otimes \rho_b(t) + O(dt); \quad (109)$$

The second term on the right hand side of this equation is the leading order term in the weak entangling of the state, and will lead, after projection, to the stochastic part of the density matrix evolution. Using the  $B$  notation has made the  $O(dt)$  size of this term explicit. To derive the deterministic part of the evolution equation we would need to keep the  $O(dt)$  terms, but since these are already known (the master equation in the Lindblad form) we will not do this here.

The scheme is now to project this density matrix onto an eigenstate of  $B + B^\dagger$  chosen with a probability given by  $P(I)$ . Because of the weak coupling of the bath with the system, this will give a small additional contribution

(actually proportional to  $\rho(t)$ ) to the system density matrix depending on the value of the current measured. Since the combination of operators  $B + B^\dagger$  is just the "displacement"  $X$  of the harmonic oscillator represented by the operator  $B$ , this projection is most easily done by first transforming the state of the bath into a Wigner function representation (see for example [19]).

At time  $t$ , the bath oscillator described by  $B(t)$  is in a thermal state and the distribution of  $X$  is a Gaussian centred at  $X = 0$  and with width  $2N_d + 1 = \coth(\hbar/2k_B T)$ . In terms of the Wigner representation in terms of coherent states  $|j\rangle$ , this state can be written as

$$W(\alpha; \alpha^*) = \frac{1}{(2N_d + 1)\pi} \exp\left[-\frac{|\alpha|^2}{(2N_d + 1)\pi}\right]; \quad (110)$$

where  $j$  is the c-number corresponding to the state  $|j\rangle$ . Following the evolution of  $W$  [26] shows that at time  $t + \Delta t$  and to  $O(\Delta t)$  the distribution of  $X$  after the evolution corresponding to the operation Eqs. (104) and (109) remains Gaussian and with the same width, but now centred around  $\frac{\hbar}{2} \text{Tr}_{(t)} [a_1 + a_1^\dagger]$ . This means that the variable  $\rho(t)X$  is a Gaussian random variable given by

$$\rho(t)X = \frac{\hbar}{2} [a_1 + a_1^\dagger] + \sqrt{\frac{\hbar}{2N_d + 1}} dW; \quad (111)$$

with  $dW$  a Wiener increment with  $dW^2 = \Delta t$ . Since the current is  $X = \rho(t)X$  this gives us the most important result, namely, that the measured current is

$$I(t) = \frac{\hbar}{2} [a_1 + a_1^\dagger] + \sqrt{\frac{\hbar}{2N_d + 1}} \dot{W}(t); \quad (112)$$

where  $\dot{W}(t) = dW/dt$  represents white noise with correlations

$$\langle \dot{W}(t) \rangle = 0; \quad (113)$$

$$\langle \dot{W}(t) \dot{W}(t') \rangle = \delta(t - t'); \quad (114)$$

Wigner's second result is for the increment of the system density matrix after evolution through  $\Delta t$  and projection by the measurement (c.f. [26] Eq. (4.113)),

$$\begin{aligned} d^{\text{st}} \rho(t) &= \hbar X_j(t + \Delta t) \rho(t) - \rho(t) X_j(t) \\ &= \frac{\hbar}{2} \frac{\rho(t)}{2N_d + 1} (N_d + 1) [a_1^{\text{st}} + a_1^{\text{st}\dagger}] - N_d [a_1^{\text{st}\dagger} + a_1^{\text{st}}] \text{Tr} [a_1^{\text{st}} + a_1^{\text{st}\dagger}] + O(\Delta t); \end{aligned} \quad (115)$$

Replacing the stochastic variable  $X$  by the expression Eq. (111), and retaining only the  $O(\Delta t)$  term gives

$$d^{\text{st}} \rho = \frac{\hbar}{1 + 2N_d} (N_d + 1) [a_1^{\text{st}} + a_1^{\text{st}\dagger}] - N_d [a_1^{\text{st}\dagger} + a_1^{\text{st}}] \frac{\hbar}{2} dW + O(\Delta t); \quad (116)$$

Equation (116) is the stochastic term that must be added to the density matrix evolution of equation (31) to give us the stochastic master equation for the density matrix conditioned on the measurement outcome.

### C. Adiabatic elimination of the stochastic master equation

Just as we did for the master equation it is possible to adiabatically eliminate the ancilla and find a stochastic master equation for the system alone. Our objective is to evaluate Eq. (116) using Eqs. (34-37). The result will lead to Eq. (132). To summarize the result, we are able to replace  $a_1^{\text{st}}$  in Eq. (116) by  $a_1$  of the deterministic calculations Eq. (50).

Since we are dealing with only the stochastic component of the stochastic master equation, we will omit the superscript "st", and we will also drop the tilde used to distinguish the density matrix with respect to displaced coordinates. We can use the result from the adiabatic elimination of the master equation to evaluate Eq. (116) and

obtain

$$\begin{aligned}
& (N_d + 1)(a_1 + \check{a}_1^y) \\
&= (N_d + 1) \left( \frac{1}{2} + \frac{1}{2} \gamma \right) N_1 \\
&+ (N_d + 1) \frac{2}{2^{2^0} + 2} + \frac{N_1}{N_1 + 1} \left( \frac{1}{2} + \frac{1}{2} \gamma \right) \check{a}_1^y N_1 + (N_d + 1) \frac{2}{2^{2^{0\gamma}} + 2} + \frac{N_1}{N_1 + 1} \left( \frac{1}{2} + \frac{1}{2} \gamma \right) N_1 a_1 \\
&+ (N_d + 1) \frac{N_1}{N_1 + 1} \left[ \frac{1}{2} + \frac{1}{2} \gamma \right] \check{a}_1^y N_1 a_1 + (N_d + 1) \frac{N_1}{N_1 + 1} \left( \frac{1}{2} + \frac{1}{2} \gamma \right) \check{a}_1^y \check{a}_1^y N_1 + (N_d + 1) \frac{N_1}{N_1 + 1} \left( \frac{1}{2} + \frac{1}{2} \gamma \right) N_1 a_1 a_1: \quad (117)
\end{aligned}$$

Similarly,

$$\begin{aligned}
& N_d (a_1^y + a_1) \\
&= N_d \left( \frac{1}{2} + \frac{1}{2} \gamma \right) \check{a}_1^y N_1 + N_d \left( \frac{1}{2} + \frac{1}{2} \gamma \right) N_1 a_1 + N_d \left( \frac{1}{2} + \frac{1}{2} \gamma \right) \check{a}_1^y N_1 a_1 + N_d \left( \frac{1}{2} + \frac{1}{2} \gamma \right) \check{a}_1^y \check{a}_1^y N_1 + N_d \left( \frac{1}{2} + \frac{1}{2} \gamma \right) N_1 a_1 a_1: \quad (118)
\end{aligned}$$

The last term in Eq. (116) can be evaluated by plugging Eq. (34) for  $\check{a}_1^y + a_1$ , then taking the trace results in leaving only the  $\left( \frac{1}{2} + \frac{1}{2} \gamma \right) \check{a}_1^y N_1 a_1$  term:

$$\text{Tr} \left( \check{a}_1^y + a_1 \right) = h_{1\gamma} + i_{1i}: \quad (119)$$

Until now, we have distinguished  $N_d$  from  $N_1$ . However, for a mesoscopic mechanical beam with current flowing through the surface of the structure,  $N_d = N_1$ . With this simplification we obtain the set of differential equations

$$\dot{r}_0 = \frac{2}{2N_1 + 1} f(N_1 + 1) \left( \frac{1}{2} + \frac{1}{2} \gamma \right) h_{1\gamma} + i_{1i} g; \quad (120)$$

$$\dot{r}_{-1} = \frac{2}{2N_1 + 1} f(N_1 + 1) \left( 2^{2^0} + 2 \right) h_{1\gamma} + i_{1i} g; \quad (121)$$

$$\dot{r}_{-1\gamma} = \frac{2}{2N_1 + 1} f(N_1 + 1) \left( 2^{2^{0\gamma}} + 2 \right) h_{1\gamma} + i_{1i} g; \quad (122)$$

$$\dot{r}_{-2} = \frac{2}{2N_1 + 1} f h_{1\gamma} + i_{1i} g; \quad (123)$$

$$\dot{r}_{-2^0} = \frac{2}{2N_1 + 1} f h_{1\gamma} + i_{1i} g; \quad (124)$$

$$\dot{r}_{-2^{0\gamma}} = \frac{2}{2N_1 + 1} f h_{1\gamma} + i_{1i} g; \quad (125)$$

where  $\dot{r}_i$  means the stochastic component only and  $\dot{r}_i = dW = dt$ .

Next we will do the adiabatic elimination as has been done for the deterministic master equation. To do the adiabatic elimination, we set off-diagonal terms in  $\dot{r}_i$  to zero. Since  $\dot{r}_i$  is actually stochastically driven as well, this is not exactly correct: strictly speaking, the stochastic terms are fluctuating. Thus in the steady state,  $r_{-1}; r_{-1}$  are not quite constant, as the adiabatic elimination assumes. However, if the fluctuation amplitude is very small (high order in  $\epsilon$ ), we can neglect the fluctuation and approximate these terms with the steady state values. Following the analysis of Doherty and Jacobs [29] we integrate the stochastic term over the time scale of the diagonal term to estimate the rms amplitude of the fluctuation.

Suppose  $f(t)$  and  $g(t)$  are arbitrary continuous functions. We show that the fluctuations of  $r_{-1}$  have a root mean square magnitude that is lower order in  $\epsilon$  than the mean over  $dW$  of  $r_{-1}$ . Thus in the steady state,  $r_{-1}; r_{-1}$  are not quite constant, as the original adiabatic elimination assumed but their fluctuations are negligible.

Consider the equation for  $\dot{r}_{-1}$

$$\begin{aligned}
\dot{r}_{-1} &= i_{01} a_0^y a_0 + \frac{N_1}{N_1 + 1} \left( \frac{1}{2} + \frac{1}{2} \gamma \right) a_0^y a_0 dt \\
&+ \frac{2}{2N_1 + 1} f(N_1 + 1) \left( 2^{2^0} + 2 \right) h_{1\gamma} + i_{1i} g dW + O(\epsilon^3) dt: \quad (126)
\end{aligned}$$

We integrate this over a time  $t = 1 =$  and use the fact that the mean values of  $\rho_{0;1}$  must be slowly varying over this time to obtain

$$\dot{\rho}_{11} = \int_0^t d_1 \quad (127)$$

$$\begin{aligned} & r \frac{N_1}{N_1 + 1} \rho_{00}^y a_0 + \frac{2}{2N_1 + 1} f(N_1 + 1) (2\rho_{00} + \rho_{11}) h_{11} + \rho_{11} i_{1g} \int_0^t dW(t^0) + O^3 : \end{aligned} \quad (128)$$

The random number  $W = \int_0^t dW(t^0)$  is Gaussian distributed with mean zero and variance  $t = 1 =$  [30], thus the root mean square size of  $W$  is  $1 =$ . As a result the stochastic term in the update of  $\rho_{11}$  is a factor of order smaller than the first term in Eq. (128) and a factor of order  $^2$  smaller than the second (damping) term. As a result the stochastic term is not of leading order and can be disregarded, leading to Eq. (50) exactly as before. We obtain  $\rho_{11}$  by taking the adjoint of  $\rho_{11}$ .

Then the stochastic part of the diagonal terms are

$$\dot{\rho}_{00} = M \mathbb{E} : + \frac{r}{2N_1 + 1} f(N_1 + 1) (\rho_{11} + \rho_{11}^y) h_{11} + \rho_{11} i_{10} ; \quad (129)$$

$$\dot{\rho}_{11} = M \mathbb{E} : + \frac{r}{2N_1 + 1} f h_{11} + \rho_{11} i_{2g} ; \quad (130)$$

where  $M \mathbb{E} .$  stands for the master equation part. Using Eq. (39) and  $i_{ij} = i_{ji}$  we obtain

$$\dot{\rho}_{ij} = M \mathbb{E} : \frac{r}{2N_1 + 1} \frac{\rho_{01j} \rho_{j01}}{j} a_0^y a_0 + \rho_{00}^y a_0 \frac{D}{2} a_0^y a_0 \rho_{ij} : \quad (131)$$

Therefore, we finally obtain the stochastic master equation (SME) for the system

$$\begin{aligned} \dot{\rho}_{ij} = & \left( \frac{\rho_{01j}^2}{2N_1 + 1} \frac{h_{ij}}{a_0^y a_0} \right) \rho_{ij} dt + \rho_{ij} \left( \frac{h_{ij}}{a_0^y a_0} \right) dt + N_0 \frac{2a_0^y}{2k} \rho_{ij} a_0 + \rho_{ij} \frac{2a_0^y}{2k} a_0 \rho_{ij} dt \\ & + \frac{p}{2k} \frac{h_{ij}}{a_0^y a_0} \rho_{ij} + \rho_{ij} \frac{2h_{ij}}{2k} a_0 i_{ij} dW : \end{aligned} \quad (132)$$

where

$$k_{ij} = \rho_{01j}^2 = (2N_1 + 1)^2 : \quad (133)$$

Using the result in Eq. (54) and the definition of  $k$  in Eq. (133), the scaled current from Eq. (112) can be expressed as

$$I(t) = \frac{p}{2N_1 + 1} \frac{D}{2} \frac{E}{2k} a_0^y a_0 + : \quad (134)$$

#### D. Analysis

As was stated previously, the first term in Eq. (132) describes the phase diffusion due to the non-linear coupling between the system and ancilla oscillators. On the other hand the final, stochastic, term reflects the effects of the measurement. Note that the coefficient of the diffusion term is just  $k$  multiplied by  $(=) (2N_1 + 1)^2$  so that the phase diffusion coefficient is enhanced over the coefficient of the term giving the effect of the measurement. This enhancement arises from the extra thermal bath connected to the ancilla that perturbs the system but is not measured, and from the inefficiency of the measurement in the presence of thermal fluctuations.

To further understand the consequences of the stochastic density matrix equation we consider a case in which the initial state is a mixture of number states,  $\rho_{ij} = \sum_n p_n |n\rangle \langle n|$ . (A thermal state is an example of such a state.) The solution of the stochastic master equation of Eq. (132) remains a mixture of number states if the initial state is a

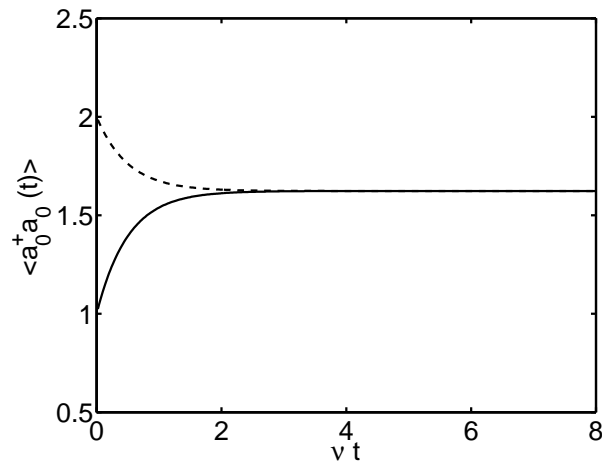


FIG. 2: A plot of Eq. (135) without the stochastic component,  $k = 0$  with the initial state  $|j_i\rangle$  (solid line) and with the initial state  $|2_i\rangle$  (dashed line).

mixture of number states. So the stochastic master equation for such an initial state can be reduced to an equation for the weights  $p_n$ , which takes the form

$$dp_n = \left[ 2(N_0 + 1)p_n - (n + 1)p_{n+1} \right] dt - \frac{p_n}{2} \sum_{n^0} \frac{X}{2k} n^0 p_{n^0} p_n dW : \quad (135)$$

Since mixtures of number states are invariant under changes of phase, neither the phase diffusion term nor the Hamiltonian terms in the stochastic master equation contribute to the evolution of the phonon number distribution. Note that this system of equations also describes the evolution of the phonon number distribution  $p_n = \langle n^j | \rho | n^j \rangle$  for an arbitrary (not necessarily diagonal) initial state  $\rho(0)$ .

The first two terms of Eq. (135) containing  $dt$  describe emission into and absorption from the thermal bath. We will see that the second, stochastic, term tends to concentrate the distribution  $p(n)$  onto a single value of  $n$ . We will discuss the competition of these tendencies in the next subsection by plotting the occupation number of the system,  $a_0^\dagger a_0(t)$ , which is given in terms of  $p_n$  by

$$\langle a_0^\dagger a_0 \rangle(t) = \sum_n n p_n(t) : \quad (136)$$

The two effects are characterized by the two characteristic time scales,  $\tau_1$  and  $k^{-1}$ , and the resulting behavior depends on the ratio of these two times.

### 1. Thermalization

Firstly we turn off the stochastic component and plot the solutions of the master equation part. Figure 2 is a plot for  $k = 0$  with the initial state  $|j_i\rangle$  and with the initial state  $|2_i\rangle$ . The thermal bath is characterized by the average occupation number  $N_0 = 1.62$ . The plot shows that the terms in  $dt$  in Eq. (135) drive the system toward a mixed (thermal) state, so that the ensemble average of  $a_0^\dagger a_0(t)$  gradually reaches the thermal average at the bath temperature. This is true regardless of the initial state. Note that the first term of Eq. (135) also describes the average over all measurement outcomes even for nonzero  $k$ .

The transition rate per unit time when the system is initially in number state  $n$  can be obtained from Eq. (135)

$$\frac{d}{dt} p_n |_{p_n(0)=1} = -2[N_0(n+1) + (N_0+1)n] : \quad (137)$$

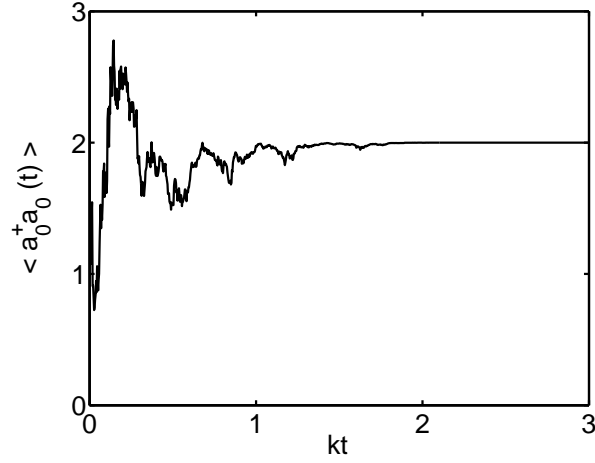


FIG. 3: A plot of a solution to Eq. (135) without the master equation component,  $\gamma = 0$  with an initial state that is thermal.

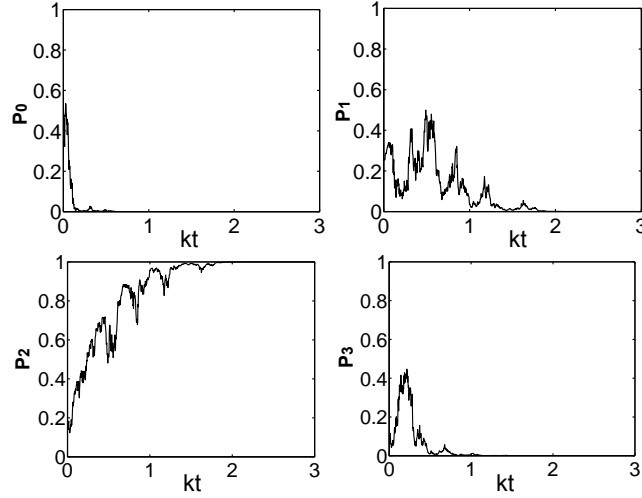


FIG. 4: Plot of  $p_n(t)$  for a simulation of Eq. (135) with  $\gamma = 0$  for the states  $|j_i\rangle; |l_i\rangle; |p_i\rangle; |b_i\rangle$ . The initial state is a thermal state with the average occupation number 1.63. The figure corresponds to Fig. 3.

The time the system resides in a given number state, which we call the dwell time  $t_{\text{dwell}}$ , can be estimated as the reciprocal of the transition rate Eq. (137)

$$t_{\text{dwell}} = \frac{1}{2 [N_0(n+1) + (N_0+1)n]} \quad (138)$$

Note that the dwell time is dependent on the state  $n$  prior to the transition. The dwell time defined here agrees well with the dwell time estimated from Fig. 2, as well as from simulations of Eq. (135) for non-zero values of  $k$ . For our measurement scheme to be useful, we want the dwell time to be long compared to the time necessary to determine which number state the system is in.

## 2. Collapse

We turn now to the measurement dynamics in the absence of thermal coupling. Figure (3) shows an example of the results of a simulation of Eq. (135) with  $\gamma = 0$ . Figure 4 shows the individual probabilities  $p_n$  for  $n = 0;1;2;3$  with an initial thermal state, which corresponds to the same simulation as in Fig. 3. All states are present initially, but eventually the system is projected onto state  $|j\rangle$ . In other runs with different random numbers for the stochastic term, different final states result, as expected. These plots show that the stochastic term tends to project the system state onto a pure number state on a time scale of order  $k^{-1}$ . We call this time the collapse time  $t_{\text{coll}}$ . Since no coupling to the thermal bath is present in these simulations, once projected, the state is stationary. The collapse onto a number state can actually be shown analytically using the solution of the system of equations (135) due to Jacobs and Knight [31].

## 3. Number state detection

Practically, another important time is the time that is needed for the measurement apparatus to distinguish one number state from the next. We call this time the measurement time.

In our model, the state of the system is monitored by the current  $I(t)$  Eq. (134). The measurement time  $t_m$  can be estimated by equating the signal  $S$ , given by averaging the current for unit phonon number  $a_0^\dagger a_0 = 1$  over the measurement time

$$S = \int_0^{t_m} dQ = \frac{p}{2N_1 + 1} \frac{p}{2kt_m}; \quad (139)$$

with the noise  $N$  over this averaging time

$$N = \frac{S}{\int_0^{t_m} dQ^2} = \frac{p}{2N_1 + 1} \frac{1}{t_m^{1/2}}; \quad (140)$$

Setting  $S=N = 1$  gives the measurement time

$$t_m = \frac{1}{8k}; \quad (141)$$

This is the time it would take to distinguish one number state from the next using the simplest possible averaging scheme, namely the integrated current. For jumps in the phonon number to be detected in the current we would need  $t_{\text{dwell}} = t_m$ . Notice that the measurement time and the collapse time are comparable. This means that if the experimenter can infer the system number state through the measurement current, then the system is actually projected to that state on the same time scale.

## 4. Collapse time versus dwell time

As we have argued above, jumps in the system number are apparent when the dwell time is longer than the collapse time so that there are plateaux in the  $a_0^\dagger a_0(t)$  curve, that is when  $t_{\text{dwell}} = t_c$ . Conversely, if  $t_{\text{dwell}} < t_c$ , transitions of the system state occur on a time scale shorter than the collapse time, so that the discrete jumps of  $a_0^\dagger a_0(t)$  become unclear.

We have simulated Eq. (135) for the cases  $t_{\text{dwell}} = t_c$  and the  $t_{\text{dwell}} < t_c$  with the fixed value of  $N_0 = 1.62$ . We use values of  $k = 250$  giving  $t_{\text{dwell}} = t_c = 153$  for state  $|j\rangle$  and  $t_{\text{dwell}} = t_c = 42.4$  for state  $|i\rangle$ , and  $k = 5$  giving  $t_{\text{dwell}} = t_c = 3.06$  for state  $|j\rangle$  and  $t_{\text{dwell}} = t_c = 0.85$  for state  $|i\rangle$ . Figures 5 and 6 show that jumps are clearly evident in the former case, but are not seen in the latter case, as expected.

We can see the jumps in the phonon number more clearly by plotting a histogram of  $a_0^\dagger a_0(t)$ . Figures 7, 8, and 9 show histograms of  $a_0^\dagger a_0(t)$  with bin width  $\Delta a_0^\dagger a_0 = 0.1$  again using a fixed value of  $N_0 = 1.62$  but with different values of  $k = 150, 15, 3$ , respectively. The clustering of the  $a_0^\dagger a_0(t)$  values around integral values is clearly evident for  $k = 150$ , is still identifiable for  $k = 15$ , and completely absent for  $k = 3$ .

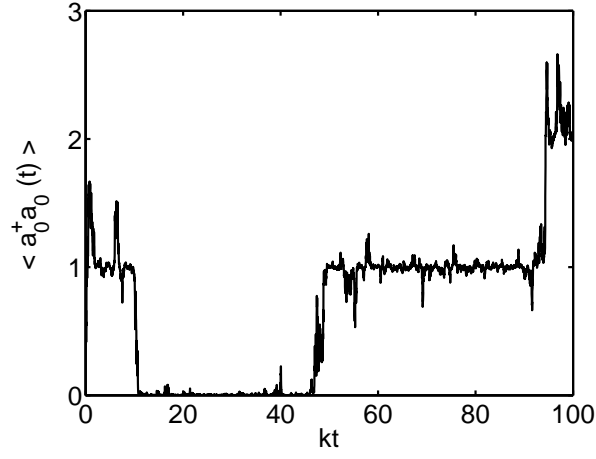


FIG . 5: The evolution of the phonon number  $\langle a_0^\dagger a_0 \rangle$  given by Eq. (135) using  $N_0 = 1:62$  and  $k= = 250$ .

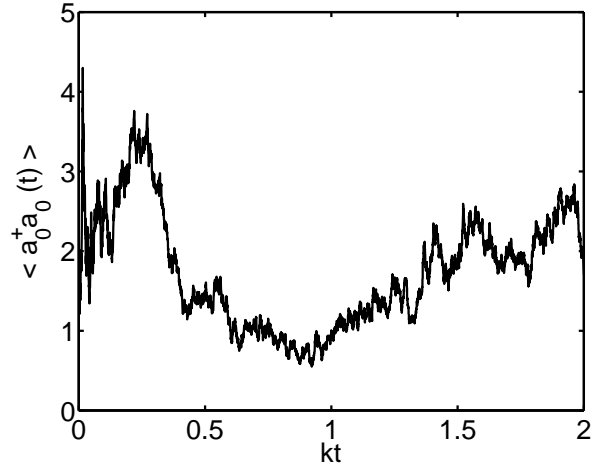


FIG . 6: The evolution of the phonon number  $\langle a_0^\dagger a_0 \rangle$  given by Eq. (135) using  $N_0 = 1:62$  and  $k= = 5$ .

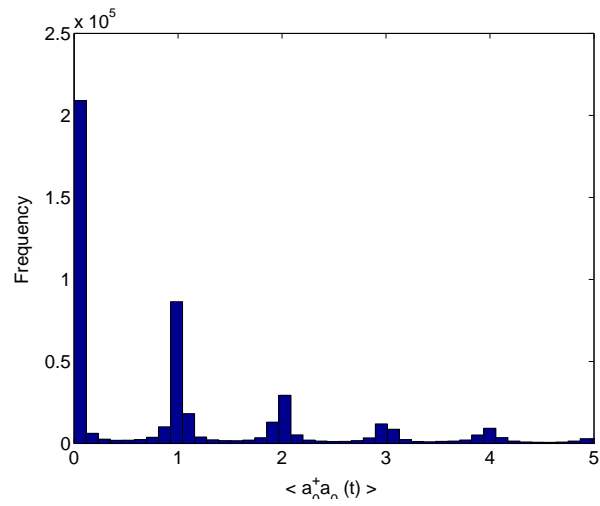


FIG . 7: A histogram of  $\langle a_0^\dagger a_0 \rangle$  for a long simulation with  $k= = 150$  and  $N_0 = 1:62$ .

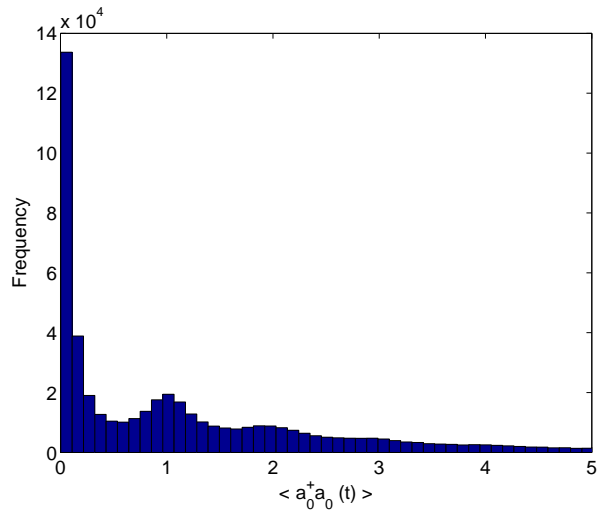


FIG . 8: As in Fig. 7 but with  $k = 15$ .

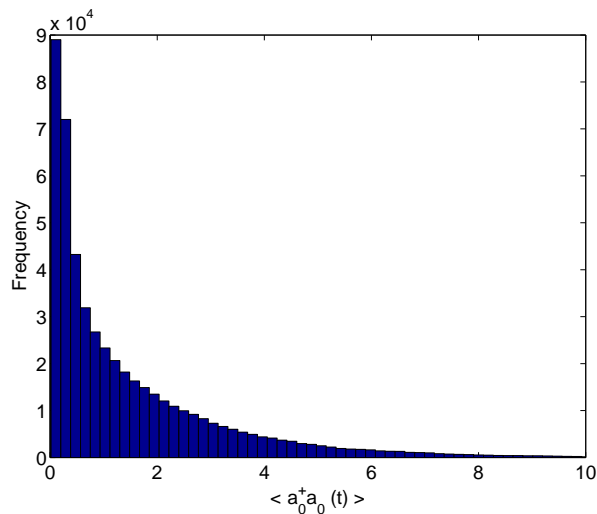


FIG . 9: As in Fig. 7 but with  $k = 3$ :

The increasing sharpness of the jumps with larger  $k = \frac{E_D}{E_D^2}$  can be seen in a more quantitative manner by plotting the deviation of the phonon number from integer values  $a_0^\dagger a_0(t) - \text{Int} a_0^\dagger a_0(t)$  as a function of  $k =$  (see Fig.10).

### 5. Effect of temperature

Since  $t_{\text{dwell}}$  is dependent on the temperature and the condition  $t_m < t_{\text{dwell}}$  effectively places a limit on the temperature of the system oscillator even for large  $k$ . Substituting Eqs. (141) and (138) for  $t_m$  and  $t_{\text{dwell}}$  and setting  $n = N_0$  in this inequality gives the condition

$$N_0(N_0 + 1) = 2k - 1 \tag{142}$$

In order to keep the same resolution for observing clear jumps as at low temperature,  $k$  must be increased as temperature increases. This is not an easy task for the experimenter: for example, an oscillator with 1 GHz resonant frequency, which is the highest frequency currently reported for a mesoscopic oscillator [3], at  $T = 0.1$  K the average occupation number is  $N_0 = 1.62$ . When the temperature is raised to  $T = 1$  K,  $N_0 = 20$ , and so if we demand the same

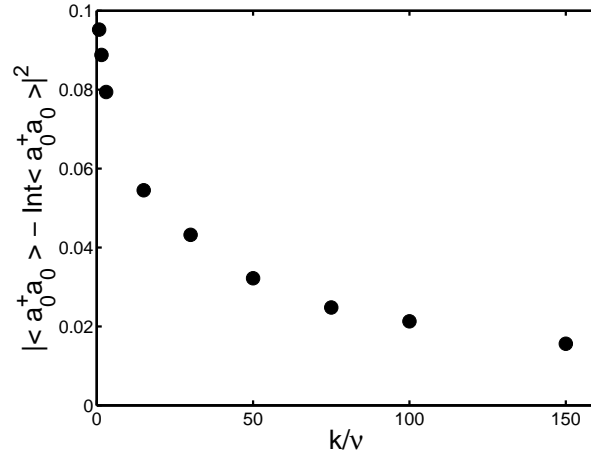


FIG. 10: The deviation of  $\langle a_0^+ a_0 \rangle$  from integral values as a function of  $k/v$ . The deviation is defined as  $|\langle a_0^+ a_0 \rangle - \int a_0^+ a_0 dt|^2$ .

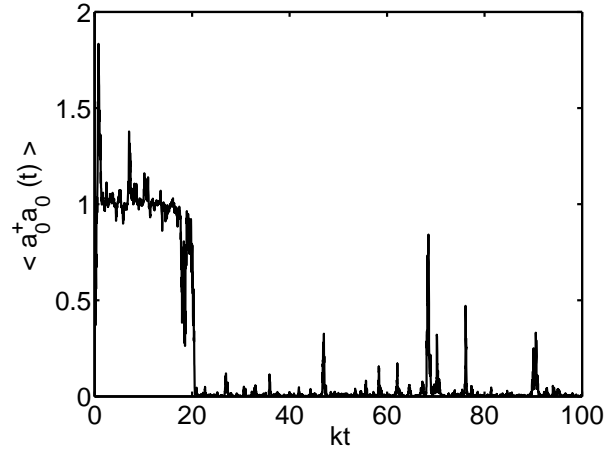


FIG. 11: Evolution of  $\langle a_0^+ a_0(t) \rangle$  at a temperature corresponding to  $N_0 = 1.62$ , with  $N_0/k = 0.0108$  and from an initial state  $|\psi_i\rangle$ .

resolution for jumping in both cases, the sensitivity of the measurement at the higher temperature must be increased by a large factor.

From Eq. (53) we can see that the transition rate depends on the temperature through the Bose distribution  $N_0$ . Figures 11 and 12 show  $\langle a_0^+ a_0(t) \rangle$  over time for different temperatures:  $N_0 = 1.62$ , for  $k/v = 150$ , and  $N_0 = 20$ , for  $k/v = 1850$ . The product  $N_0/k$  has been kept constant at 0.0108 in order to provide the same resolution for the jumps. The plots show that for the higher temperature the transitions occur more frequently. In Fig. 12, the transitions occur so rapidly that it is not easy to see the jumps on the time scale plotted. Also notice from Eq. (138) that  $t_{\text{dwell}}$  decreases with the system state  $n$  making it difficult to recognize the discrete jumps when the system state is at higher  $n$ :

#### E. Filtering the measurement current

We have seen before that the quantum trajectory equations provide a way to perform a simulation by picking the measurement results  $I(t)$  with the correct probability distribution and following the corresponding evolution of the

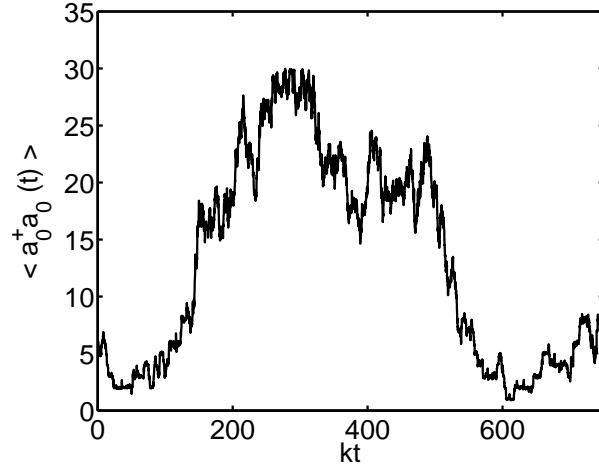


FIG. 12: Evolution of  $\langle a_0^\dagger a_0 \rangle$  at a higher temperature than in Fig. 11 corresponding to  $N_0 = 20$ , again with  $N_0/k = 0.0108$ , and from an initial state  $|\Phi_i\rangle$ .

system state. However an important point about the relation between trajectories and experimental outcomes is that in principle one can use the trajectory approach to reconstruct the dynamics of the system given the initial ensemble  $\rho_s(t_0)$  and the measured current  $I(t)$ . This can be seen more readily if we rewrite Eq. (134) as

$$dW = \frac{1}{2N_1 + 1} \sum_n I(t) \frac{p}{2k} \frac{D}{a_0^\dagger a_0(t)} dt; \tag{143}$$

Our calculation in the previous section shows that in each time-step the probability distribution for  $I(t)$  is Gaussian with mean  $\langle a_0^\dagger a_0 \rangle$  and variance  $\frac{1}{(2N_1 + 1)k} = \frac{1}{2k}$ . In our simulations we draw  $I(t)$  at random from this distribution and find the stochastic density matrix  $\rho_s$  by projecting the output field onto the corresponding current eigenstate. Alternatively, if  $I(t)$  results from experimental data, the experimenter can in principle propagate Eq. (143) and then can estimate the phonon number at each time by  $\langle a_0^\dagger a_0 \rangle = \text{Tr} [a_0^\dagger a_0 \rho_s]$ . This procedure, which goes from the measured  $I(t)$  to a deduced  $\langle a_0^\dagger a_0 \rangle$  is a kind of low pass filtering that could be performed by the experimenter to reduce the noise in the measurement. Quantum trajectories can be regarded as an optimal filter for the current, and  $\langle a_0^\dagger a_0 \rangle$  obtained from these trajectories contains the minimal amount of noise due to the measurement apparatus.

A simpler but not necessarily optimal procedure is to use a low-pass filter on  $I(t)$  with the bandwidth designed to pick out the transitions between number states. We show the results of doing this with a simple moving average filter with varying averaging windows in Fig. 13.

For the window sizes  $kt$  equal to 4.5 or 7.5 the noise averaging is sufficient to display the steps in  $\langle a_0^\dagger a_0 \rangle$  without too much rounding of the transitions.

## VI. PARAMETERS AND CONSTRAINTS

The results of the previous section show that a large value of the ratio  $k=$  is crucial for the observation of single quantum jumps in the phonon number. This ratio depends on the following adjustable parameters that characterize the experimental apparatus:

- $N_1$  =  $\langle n_{11} \rangle$
- $N_0$  =  $\langle n_{00} \rangle$
- $\alpha_1$  anharmonic coupling coefficient
- $\gamma$  damping rate for system oscillator
- $\gamma_0$  damping rate for ancilla oscillator
- $j$  mean phonon number of ancilla

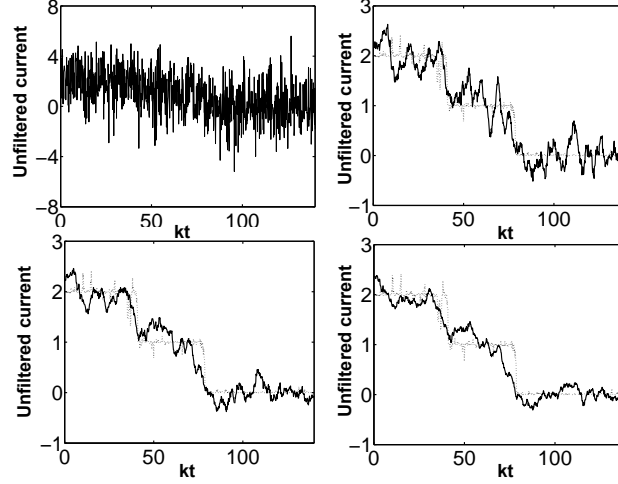


FIG. 13: Filtered current using a running average over various window sizes, for parameters  $k = 250$  and  $N_0 = 1:62$ . The dotted line is  $\langle a_0^\dagger a_0 \rangle(t)$  given by the stochastic density matrix. The current was first averaged over a time interval of  $k \tau = 0:15$ . Upper left: current observed; upper right: window size  $k \tau = 4:5$ ; lower left: window size  $k \tau = 7:5$ ; lower right: window size  $k \tau = 10:5$ .

To analyze the interplay of the parameters, we simplify the expression for  $k =$  by assuming that most of the damping of the ancilla comes from the necessary coupling to the measurement device, rather than from the external bath, i.e.  $\gamma = \gamma_0$ . Then using the expression of  $k$  from Eq. (133) and  $\gamma_0 = \omega_0 = 2Q_0$  we get

$$\frac{k}{\omega_0} \approx \frac{4(2N_d + 1)^{-1} Q_0 Q_1 \omega_1}{\omega_0} \frac{\omega_1}{\omega_0} \omega_1^2 |j_j|^2 \quad (144)$$

Equation (144) shows that the success of the measurement procedure is favored by large oscillator  $Q$ -factors, large driven response  $|j_j|^2$  and a large value of the anharmonicity coupling factor  $\omega_1 = \omega_1$ . In addition, as we have seen, detecting individual jumps becomes harder as the temperature increases. Increasing the  $Q$ -factors of mesoscopic oscillators is an active area of research. Currently, values of order  $10^3$  to  $10^4$  seem possible. If these could be raised to the values characteristic of more macroscopic oscillators of the same material, of order  $10^6$  or even higher, the detection of individual phonons would become correspondingly easier. The frequency ratio  $\omega_1 = \omega_0$  appearing in Eq. (144) must be less than unity for our detection scheme, but will probably not be too small because of geometry constraints. Thus the main parameters available to optimize the experimental geometry are the anharmonicity factor  $\omega_1 = \omega_1$  and the dimensionless measure of the driven displacement of the ancilla,  $|j_j|^2$  (the number of phonons in the driven state). We now consider these factors in more detail.

#### A. Anharmonicity Coefficient

The interaction Hamiltonian for the system and ancilla oscillators Eq. (11) can be written

$$H^{RW A} = \omega_0 a_0^\dagger a_0 + \omega_1 [n_1 + \omega_1 n] a_1^\dagger a_1; \quad (145)$$

with  $n$  the system phonon number. This equation implies that  $\omega_1$  can be estimated as the frequency shift of the ancilla oscillator for a single quantum ( $n = 1$ ) of the system oscillator.

For the prototype geometries using the two orthogonal flexing modes of a single beam, or parallel flexing modes of two longitudinally coupled beams, the nonlinear coupling arises from geometrical effects. At second order, the transverse displacement in one mode gives a longitudinal strain, which then changes the frequency of the second mode. The strain generated by the flexing motion and the frequency shift associated with this strain can be derived using elasticity theory, and have been calculated by Harrington and Roukes [32]. A demonstration of such frequency

shift detection, and direct measurement of  $\omega_{01}$  between two coupled beams has recently been reported [33]. In the small angle approximation the longitudinal strain produced by a single quantum in the fundamental exciting motion is

$$\epsilon \sim \frac{1}{m_0 \omega_0^2 L_0^2}; \quad (146)$$

where  $m_0$  is the mass and  $L_0$  is the length of the system beam. Then the ancilla frequency shift caused by this strain is

$$\omega_{01} = \beta_1 \frac{I_1^2}{2^2 d_1^2}; \quad (147)$$

where  $\beta_1$  is a geometric factor ( $\beta_1 = 3$  for clamped beam boundary conditions) and  $I_1; d_1$  are the length and thickness of the ancilla beam, respectively. Introducing a dimensionless quantity,

$$R = \frac{\beta_1^2}{m_1 d_1^2} \frac{1}{\omega_1^2}; \quad (148)$$

then the scaled coupling coefficient can be expressed as

$$\frac{\omega_{01}}{\omega_1} = \frac{m_1 \beta_1 I_1^2}{2^2 m_0 \omega_0^2 L_0^2} R; \quad (149)$$

Since the factor that is the ratio of the two mode parameters will not be too large or small, the most important quantity determining the anharmonicity factor, which must not be too small for the success of the measurement scheme, is the dimensionless ratio  $R$ . This will typically be a small number. The need for small devices is seen from the scaling of this parameter with the dimensions.

#### B. Driving strength

The detection scheme we have considered is to measure the phase of the driven response of the ancilla oscillator. Since the detection scheme is magnetomotive, it is natural to consider the use of magnetic driving in estimating the size of the displacement parameter  $j_j$ . For magnetic driving using a current  $I_{\text{drive}}$  in a magnetic field  $B$  the dimensionless displacement can be estimated as

$$j_j = Q_1 \frac{B I_{\text{drive}} L_1 d_1}{2^2 \omega_1^2} \frac{1}{R}; \quad (150)$$

Again the important role of  $R$  in limiting the size of  $j_j$  in this analysis is apparent.

We must also recognize that the size of  $j_j$  might be limited by other physical constraints, rather than by the available drive strength. One constraint might be to avoid undesired nonlinear effects in the driven beam itself. For a classical oscillator, at sufficiently large drive amplitudes nonlinear frequency pulling leads to a multiplicity of solutions and instability. This occurs when the nonlinear frequency shift is comparable with the width of the resonance  $\omega_1 = Q_1 \gamma$ . Using the same type of estimate for the nonlinear frequency shift as in Eq. (147) shows that this occurs for

$$j_j \lesssim \frac{1}{Q_1 R}; \quad (151)$$

The importance of this classical estimate to the quantum oscillator is not clear, and a more detailed, quantum mechanical analysis of the driven nonlinear oscillator will be presented elsewhere.

#### C. Example Configuration

As a first estimate of the order of magnitude of the quantities introduced above we will construct an example configuration using parameters that seem plausible with current technology.

Recently, oscillators with resonant frequencies as high as 1 GHz have been fabricated [3] using silicon carbide. Thus we consider two exciting modes of with resonant frequencies of  $\omega_0 = 2.3$  GHz and  $\omega_1 = 0.36$  GHz so that  $\omega_0 / \omega_1 \approx 6.4$ ; will be satisfied. For this value of the system oscillator frequency,  $\omega_0 / \omega_1 \approx k_B T$  is unity at a

temperature of about 0.1 K. The oscillators in Ref. [3] were not very small, but it is expected that the structure can be scaled down while maintaining the high oscillation frequency. We therefore suppose smaller dimensions consistent with these frequencies, namely dimensions are 0.63  $\mu\text{m}$   $\times$  0.04  $\mu\text{m}$   $\times$  0.07  $\mu\text{m}$  for the system beam and 0.6  $\mu\text{m}$   $\times$  0.04  $\mu\text{m}$   $\times$  0.01  $\mu\text{m}$  for the ancilla beam. With these parameters we obtain

$$R = 3.84 \times 10^9 : \quad (152)$$

The factor  $R$  occurs squared in  $k_{\text{eff}}$  (via Eq. (149), which is required to be large, and so this small factor must be mitigated by the other quantities in Eq. (149), i.e. large  $Q$ -factors and large driven amplitude  $j_j$ . Suppose the  $Q$ -factor of the system oscillator is  $Q_0 = 10000$  and  $Q_1 = 1000$ . For the size of  $j_j$  first consider the magnetic driving. A magnetic field  $B = 10$  Tesla and  $I_{\text{drive}} = 1$  A can raise the driven response to  $j_j \sim 10^6$ . To reach  $k_{\text{eff}} \sim 1$  the nonlinear coupling  $\kappa_{01} = \kappa_{10}$  that is required is then

$$\kappa_{01} = \kappa_{10} = 5.2 \times 10^8 : \quad (153)$$

With the given beam dimensions and the geometric nonlinearity, the anharmonic coupling coefficient is actually  $\kappa_{01} = \kappa_{10} = 1.1 \times 10^{11}$ , about three orders of magnitude smaller. One possible way to increase this value might be to engineer the geometry of the oscillator so that the anharmonic coupling is larger than in the simple geometric nonlinearity we have considered [35]. Another way to increase  $k_{\text{eff}}$  is to increase  $j_j$  using a different driving scheme, although for the value of  $R$  in Eq. (152) the limit in Eq. (151) is already exceeded for  $j_j \gg 10^3$ , so that engineering the geometry to reduce the self-nonlinearity might be necessary. An obvious way to increase  $k_{\text{eff}}$  to values greater than unity is to use oscillators with smaller dimensions, for example carbon nanotubes.

## VII. CONCLUSION

We have proposed and analyzed a scheme to observe quantum transitions of a mesoscopic mechanical oscillator. The non-linear coupling shifts the frequency of a second (ancilla) oscillator proportionally to the excitation level of the first (system) oscillator. This frequency shift may be detected as a phase shift of the ancilla oscillation when driven on resonance. In principle, a QND measurement is possible if the coupling constant between the two oscillators  $\kappa_{01}$  is much smaller than the resonance frequencies of the oscillators. We have derived the master equation for the system density matrix first integrating out the environment and measurement degrees of freedom, and then by removing the ancilla operator using the fact that the time scale of the system and ancilla dynamics are quite different. The master equation has three components: phase diffusion as a result of the measurement backaction; a constant energy shift due to the excitation of the ancilla oscillator, and number state transitions due to the interaction with the thermal bath (the environment).

Measurements introduce a stochastic component into the system dynamics and we have obtained the stochastic master equation corresponding to our measurement scheme. This process is called unravelling the master equation. From the stochastic master equation we identify two competing tendencies that can be characterized by two parameters. One is the coupling strength of the system and thermal bath, which is associated with the dwell time  $\tau_{\text{dwell}}$  between transitions. The other is the coefficient  $k$ , associated with measurements, which includes not only the coupling strength of the system to the bath but also the anharmonic coupling strength between the oscillators, the driving amplitude, and the sensitivity of the measurement apparatus. This coefficient is related to the measurement time  $\tau_m$  that is needed for a measurement to be able to produce an outcome with certainty. To observe clear quantum jumps we would need  $\tau_{\text{dwell}} \ll \tau_m$ . If this condition is not satisfied, then the experimenter cannot infer the energy eigenstate of the system from the observed current.

Although our simple estimates based on plausible lithographically prepared oscillators yield values for the ratio  $\tau_{\text{dwell}} = \tau_m$  too small for the observation of individual phonons, enhancements to the geometry considered and the trend to smaller device sizes should improve the outlook. The basic scheme and theoretical techniques developed here are fairly general, and in particular are not restricted to zero temperature, and so can be also used for other applications such as a single spin detection and noise analysis for a solid state based quantum computer. Such possibilities might open up a new stage for observing quantum dynamics in mesoscopic systems.

## Acknowledgments

DHS acknowledges Michael Rourke for discussions and support of this work. DHS also thanks Gerard Milburn for discussions and is grateful to the SRC for Quantum Computer Technology at the University of Queensland for their hospitality during the extensive stay. In addition, DHS is also grateful to Tony Leggett for discussions. Furthermore,

DHS acknowledges the Weitzman fund for a travel grant. We thank Michael Rourke for providing information about the experimental progress in his group. This work is supported by DARPA DSO/MOSAIC through grant N00014-02-1-0602 and NSF through grant DMR-9873573. Work by ACD was supported by the NSF through grant EIA-0086083 as part of the Institute for Quantum Information and the Caltech URICenter for Quantum Networks (DAAD 19-00-1-0374).

- 
- [1] Adrian Cho, *Science*, 299, 36 (2003).
- [2] M. L. Rourke, *Physics World*, 14, 25 (2001).
- [3] X. M. H. Huang, C. A. Zornan, M. Mehregany and M. L. Rourke, *Nature*, 421 (6922), 495 (2003).
- [4] V. B. Braginsky and F. Ya. Khalili, *Quantum Measurement*, Cambridge University Press, Cambridge (1995).
- [5] B. Yurke, *Personal Communication*.
- [6] L. D. Landau and E. M. Lifshitz, *Theory of Elasticity*, Butterworth-Heinemann, Oxford (1986).
- [7] S. Timoshenko, *Theory of Elastic Stability*, McGraw-Hill, New York (1991).
- [8] S. M. Carr, W. E. Lawrence, and M. N. Wybourne, *Physica B*, 316, 464 (2002).
- [9] C. M. Caves, K. S. Thorne, R. W. P. Drever, V. D. Sandberg, and M. Zimmermann, *Rev. Mod. Phys.* 52 (2), 341 (1980).
- [10] D. F. Walls and G. J. Milburn, *Quantum Optics*, (Springer-Verlag, Berlin, 1995).
- [11] B. Yurke, D. S. Greynall, A. N. Pargellis, and P. A. Busch, *Phys. Rev. A* 51 (5), 4211 (1994).
- [12] A. N. Celand and M. L. Rourke, *Appl. Phys. Lett.* 69, 2653 (1996).
- [13] A. N. Celand and M. L. Rourke, *Sensors and Actuators A*, 72, 256 (1999).
- [14] B. Yurke and J. S. Denker, *Phys. Rev. A* 29, 1419 (1984).
- [15] W. H. Louisell, *Quantum Statistical Properties of Radiation*, Wiley Classics Library Wiley, New York, (1990).
- [16] R. E. S. Polkinghorne and G. J. Milburn, *Phys. Rev. A* 64, 042318 (2001).
- [17] C. M. Caves, *Phys. Rev. D* 26, 1817 (1982).
- [18] J. M. Courty, F. Grassia and S. Reynaud, *Europhys. Lett.* 46, 31 (1999).
- [19] C. W. Gardiner and P. Zoller, *Quantum Noise*, 2nd ed., (Springer-Verlag, Berlin 2000).
- [20] H. M. Wiseman and G. J. Milburn, *Phys. Rev. A* 47 (1), 642 (1993).
- [21] P. W. arszawski and H. M. Wiseman, *Phys. Rev. A* 63 (1) 013803 (2001).
- [22] D. F. Walls and G. J. Milburn, *Phys. Rev. A* 31, 2403 (1985).
- [23] A. Barchielli, *Phys. Rev. A* 34 (3), 1642 (1986).
- [24] A. Barchielli, *J. Phys. A* 20, 6341 (1987).
- [25] H. Carmichael, *An Open System's Approach to Quantum Optics*, Springer-Verlag, Berlin, (1993).
- [26] H. M. Wiseman, PhD Thesis, University of Queensland, St. Lucia (1994).
- [27] M. B. Plenio and P. L. Knight, *Rev. Mod. Phys.*, 70, 101 (1998).
- [28] T. A. Brun, quant-ph 0108132 (2001).
- [29] A. C. Doherty and K. Jacobs, *Phys. Rev. A* 60 (4) 2700 (1999).
- [30] C. W. Gardiner, *Handbook of Stochastic Methods*, (Springer-Verlag, Berlin 1985).
- [31] K. Jacobs and P. L. Knight, *Phys. Rev. A* 57, 2301 (1998).
- [32] D. A. Harrington and M. L. Rourke, *Caltech Technical Report CMP-106* (1994).
- [33] X. M. H. Huang, M. K. P. Rakash, B. Yurke, and M. L. Rourke, to be published.
- [34] C. W. Gardiner, A. S. Parkins, and P. Zoller, *Phys. Rev. A* 46 (7) 4363 (1992).
- [35] M. L. Rourke, *Personal Communication*.
- [36] L. D. Landau and E. M. Lifshitz, *Mechanics*, Butterworth-Heinemann, Oxford (1986).
- [37] Actually, it is not necessary to make the rotating wave approximation with respect to both oscillators as the interaction  $V_{anh}$  becomes QND after the rotating wave approximation made in an interaction picture with respect to  $\sim!_0 a_0^\dagger a_0$  only. However, we make the further rotating wave approximation to simplify the later development.
- [38] The detailed analysis of non-linearities of the system and ancilla internal Hamiltonian and the correction to the dynamical equation due to these terms will be discussed elsewhere.
- [39] However, the driving strength is chosen in such a way to avoid the bi-stability region caused by the anharmonicity of the oscillator, see VI.
- [40] It can be shown that  $\rho = \sum_{h, h', i, i'} a_0^\dagger a_0; a_0^\dagger a_0; \dots$  can be rewritten in coherent state representation as  $\rho_Q = \int d\theta d\phi \dots \rho^2_Q = \rho^2$ , where  $Q$  is the  $Q$ -representation density matrix [19] and  $\theta$  is the phase of the coherent state. This equation shows the diffusion of the phase variable.